SHAPE-MEMORY EFFECT IN A Cu-Al-Ni ALLOY

by

EROL SELİMBEYOĞLU

B.S. in M.E., Boğaziçi University, 1983

Submitted to the Institute for Graduate Studies in Science and Engineering in partial fulfillment of the requirements for the degree of

Master of Science

in

Mechanical Engineering

Boğaziçi University

1986

SHAPE-MEMORY EFFECT IN A Cu-Al-Ni ALLOY

APPROVED BY

Doç. Dr. Sabri ALTINTAŞ
(Thesis Advisor)

S. Altıntaş

Doç. Dr. Gülay AŞKAR

Doç. Dr. Sabri KAYALI

S. Kayalı

DATE OF APPROVAL: 10.8.1986

ACKNOWLEDGEMENT

I would like to express my most sincere appreciation to my thesis supervisor Doç. Dr. Sabri ALTINTAŞ for his most helpful advice and guidance throughout the course of this work.

I also wish to express my gratitude to Prof. Dr. Şefik GÜLEÇ, Head of the Material Research Department, for permission to carry out this research in TUBİTAK.

My grateful appreciation goes to Mr. Nüshan ERDEM for his invaluable assistance in building apparatus, to Mr. Suat TUNCEL for the photography, and to Mr. Mehmet DEMİRKOL in making the tests.

Finally, I wish to thank all technical staff of the Material Research Department for their assistance.

February, 1986 Erol SELİMBEYOĞLU

SHAPE-MEMORY EFFECT IN A Cu-Al-Ni ALLOY

ABSTRACT

In this study, the microstructure and mechanical property relationship of Cu-13.98Al-2.94Ni (wt.pct.) alloy that exhibits shape-memory effect is investigated.

A brief review of thermoelasticity, pseudoelasticity, and memory effects are presented together with the complementary relationship of shape-memory effect and pseudoelastic effect. Then the mechanical behaviour, mechanisms, and some applications of shape-memory alloys are given. After these, the Cu-Al-Ni alloy system is explained in detail.

In the experimental work, the Cu-Al-Ni alloy system is produced and the mechanical properties are measured with bending and hardness testing. The microstructures are examined using the techniques of optical microscopy. For the present alloy, room temperature is between M_s and A_s. Therefore, it is either in the parent phase or in the martensitic state at room temperature. The shape-memory effect occured on deformation in both states. Deformation caused the formation or reorientation of the martensite plates depending on the initial position of the alloy. When the specimen was heated, the martensite plates formed in both states disappeared and the specimen reverted back to its original shape.

Ö Z E T

Bu çalışmada şekil-bellek özelliği gösteren Cu-%13.98Al-%2.94Ni alaşımının mekanik özellikleri ve mikroyapısı arasındaki ilişki incelenmiştir.

Termoelastisite, pseudoelastisite ve şekil-bellek özelliklerinin kısa bir özeti, şekil-bellek etkisi ve pseudoelastik etki arasındaki tamamlayıcı ilişki ile birlikte sunulmuştur. Daha sonra sırası ile şekil-bellekli alaşımların mekanik davranışları, mekanizmaları, bazı uygulamaları verilmiş ve Cu-Al-Ni alaşım sistemi ayrıntılı bir şekilde incelenmiştir.

Deneysel çalışmada Cu-Al-Ni alaşım sistemi üretilmiş, mekanik özellikleri eğme ve sertlik deneyleri ile ölçülmüş olup, elde edilen yapılar optik mikroskop kullanılarak incelenmiştir. Oda sıcaklığı alaşımın M_S ve A_S sıcaklıkları arasında kalmaktadır, bu nedenle alaşım oda sıcaklığında ana faz durumunu ya da oluşturulan martenzit yapısını koruyabilmektedir. Nümune her iki durumda da deformasyona uğratıldığında şekil-bellek özelliği göstermiştir. Deformasyon martenzit oluşumuna ya da başlangıçta termoelastik olarak oluşturulan martenzitin yeniden düzenlenmesine neden olmuştur. Daha sonra nümune ısıtıldığında her iki durumda da oluşturulan martenzit tabakaları kaybolmuş ve nümune ilk şeklini almıştır.

TABLE OF CONTENTS

LIST OF FIGURES

Page

Page

LIST OF TABLES

LIST OF SYMBOLS

M_s	:	The temperature at which martensite starts forming.
M_f	:	The temperature at which martensite completes its forming.
A_s	:	The temperature at which parent phase starts forming.
A_f	:	The temperature at which parent phase completes its forming.
M_d	:	The temperature below which martensite can be stress induced from the parent phase.
SME	:	Shape-memory effect.
TWSME	:	Two-way shape-memory effect.
SIM	:	Stress induced martensite.
Nitinol	:	Ni-Ti Naval Ordnance Laboratory.

I. INTRODUCTION

Recently, the shape-memory effect - so called shape-memory alloys - and associated characteristics such as the two-way shape-memory, pseudoelasticity, and mantensite-to-mantensite transformations have attached much interest [1-7]. If one bends, for example, a wire of this memory alloy, it becomes straight again on heating. As a result of further research, additional processes have been discovered in which, after the first deformation, a reversible shape change on heating and successive cooling is also obtained. This phenomenon is described as the two-way memory effect because the shape change occurs both on heating and cooling. Shape-memory alloys, notably those of the Ni-Ti type and the copper-based types are now used in a variety of commercial applications such as couplings, fittings and numerous actuators. The Ni-Ti alloys are also finding use in medical and dental applications [8].

It was not until 1962 that the phenomenon came to worldwide attention with the announcement of shape-memory in Ni-Ti alloy system. The alloy was discovered by W.J. Buehler et al [2] of the U.S. Naval Ordnance Laboratory. These so called Nitinol alloys (Ni-Ti-Naval-Ordnance-Laboratory) with approximately equiatomic Ni-Ti showed an

unusual mechanical memory as a function of deformation and temperature.

Not all metals exhibit a memory effect, because the prerequisites are only given in certain alloy systems. Table I [3] gives the alloy systems which have so far been investigated. Prerequisites for the shape-memory behaviour have been investigated by many workers [9-12].

TABLE 1 - List of Alloys Showing Memory-Effect [3]

Thermoelastic	Shape-Memory Effect
Fe-Pt	In-Cd
Cu-Al-Ni	Ti-Nb
Cu-Zn	304 stainless steel
Cu-Zn with ternary additions of Ni,Ag,Au,Cd,In,Ga,Si,Ge,Sn,Sb	Ni-Al
Ag-Cd	Cu-Zn
Ti-Ni	Ag-Cd
Au-Cu-Zn	Fe-Ni
Ni-Al	Ni-Ti
	Cu-Al
Pseudoelastic	Cu-Al-Ni
	Ti-Ni
Cu-Zn	Au-Cd
Cu-Zn-X	In-Tl
Cu-Zn-Sn	Fe-Pt
Cu-Al-Ni	Au-Cu-Zn
Cu-Al-Mn	Cu-Zn-Si
Ag-Cd	Cu-Zn-Sn
Au-Cd	Cu-Sn
Cu-Au-Zn	Fe-Mn-C
Fe_3Be	Ni-Ti-X (X-ternary element)
Fe_3Pt	Cu-Zn-Al
In-Tl	Cu-Zn-Ga
Ni-Ti	Cu-Au-Zn
Ti-Ni	
Au-Cu-Zn	Two-way Shape-Memory Effect
Cu-Sn	
	In-Tl
	Ti-Ni
	Cu-Al
	Te-Mn-C
	Cu-Zn
	Ni-Al
	Cu-Al-Ni
	Cu-Zn-Al

According to K. Otsuka [10] the necessary conditions for the shape-memory effect are as follows:

a. the martensitic transformation is thermoelastic.
b. the parent and martensitic phases are ordered.
c. the lattice invariant strains in the martensitic phase are not due to dislocations but twins or stacking faults.
d. if the ordering is disregarded, the matrix phase has a BCC structure and the martensite phase a HCP structure.

In the absence of stress, martensites start forming at a particular temperature M_s on cooling, and is completed at some lower temperature M_f. The reverse transformation begins and ends at the corresponding temperatures A_s and A_f. The martensite can also be formed above but close to M_s temperature by the application of a suitable stress. M_d is the temperature below which martensite can be stress induced from the parent phase.

Some of terminology used in this field are as follows:

a) "Thermoelastic Martensitic Transformation": A martensite forms and grows continuously as the temperature is lowered and shrinks and vanishes as the temperature is raised.

b) "Pseudoelastic Effect": The specimen recovers a proportion of the induced strain immediately on unloading.

c) "Shape-Memory Effect (SME)": A specimen which has been deformed maintaines that deformation when the applied stress is removed, but recovers its original shape when heated.

d) "Two-Way Shape-Memory Effect (TWSME)": A specimen changes shape in both directions as a function of temperature (heating and cooling) remembering both high and low temperature shapes.

Some terms used in this study may be used with different names in other papers. Table II [3] gives a comparative compilation of terms and Figure 1 [3] illustrates the above mentioned effects schematically.

TABLE II - A Comparative Compilation of Terms [3]

Terms in this study	Terms used in other papers
Thermoelastic (transformation)	thermoelastic (transformation)
Pseudoelasticity	superelasticity metalelasticity rubberlike behaviour stress-induced pseudoelasticity (STRIPE) elastic shape-memory effect ferroelasticity anelastic strain recovery anomalous elongation due to martensitic transformation
Shape-memory effect (SME)	plastic shape-memory effect marmem strain memory effect annihilation effect of martensitic shears
Two-way shape-memory effect (TWSME)	reversible memory reversible linear change on transformation reversible shape-memory effect

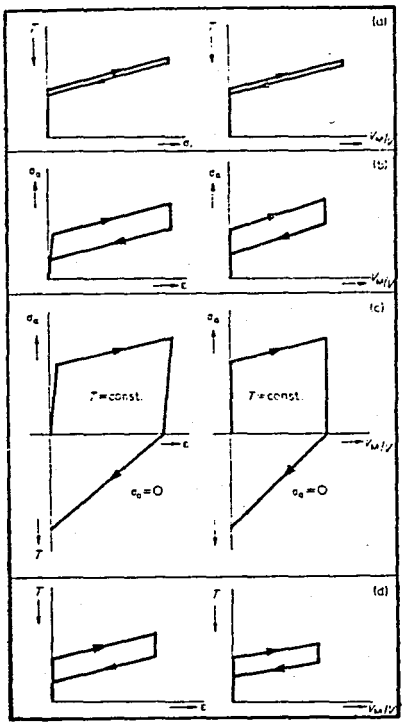

Figure 1 - (a) Schematic representation of the formation and reverse transformation of thermoelastic martensite as a function of temperature; σ_1 represents the internal stresses arising by the transformation. V_M/V the fractional volume of the martensite product. (b) Schematic representation of pseudo-elasticity. Martensite forms as the applied stress is increased producing the macroscopic strain. Release of stress causes the martensite to revert to the parent phase. (c) Schematic representation of shape-memory effect. Martensite is formed by straining but remains stable upon removal of the external stress; it is reverted to the parent phase on heating. (d) Schematic representation of two-way memory effect. On cooling macroscopic strain is produced without the application of an external stress; the strain disappears again on increasing the temperature [3].

The purpose of the present investigation is summarized as follows:

a. to produce a Cu-Al-Ni alloy system which exhibits shape-memory effect;

b. to correlate the structural changes with load-deflection curves after unloadings;

c. to examine the hardness values obtained after each stage of production and in both parent and martensitic states.

In the following, Section II a brief review of the important results obtained in previous studies will be given. Next, in Section III Cu-Al-Ni alloy system which is the subject of the present study will be presented. In Section IV experimental work and the results of this study and in Section V comparison of some important observations with other studies will be given. In the last section, the conclusions of the study will be presented.

II. SHAPE-MEMORY ALLOYS

Considerable attention has been paid in the literature to the various shape-memory effects and these have been reviewed in detail by many workers [1,13-16] in the past years. Recent studies of the shape-memory effect in alloys forming thermoelastic martensites with various crystal structures have shown that a somewhat universal behaviour exists [17]. Before focusing on the Cu-Al-Ni alloy system, the literature pertaining to the microstructural features of thermoelasticity, pseudoelasticity and memory effects associated with martensitic transformations will be reviewed. The interrelations between the various effects will be described. Then the mechanical behaviour, mechanisms and some applications of the shape-memory alloys will be given.

2.1 THERMOELASTICITY

A thermoelastic martensitic transformation is one in which the martensite plates form and grow continuously as the temperature is lowered and disappear by the exact reverse path as the temperature is raised as shown in Figure 2 [3]. Figure 1(a) gives a schematic

representation of this transformation by indicating the increase in internal stress, σ_i (stored elastic energy) and the fractional increase in the amount of martensite as measures of the progress of transformation, and the decrease of these properties due to reverse transformation.

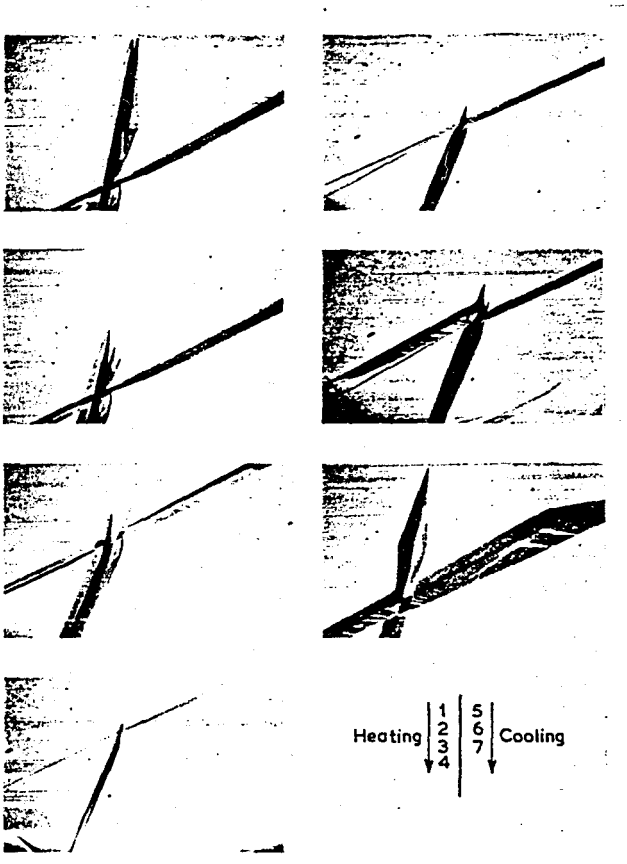

Figure 2 - Thermoelastic behaviour in AgCd showing the growth of self-accommodating groups [3].

There is no sudden appearance or disappearance of large groups of plates (burst). The formation of martensites proceeds by the continuous growth of martensite plates and the nucleation of new plates on cooling. When cooling is stopped; growth ceases, but resumes upon subsequent cooling until the martensite plates impinge

with each other or with grain boundaries. Upon heating the reverse martensite-parent transformation occurs by the backwards movement of the martensite/parent interfaces; the plates of martensite simply shrink and revert completely to the parent phase in its original orientation.

The transformation proceeds essentially in equilibrium between the chemical driving energy of the transformation and a resistive energy whose dominating component is the stored elastic energy. Thus the transformation is defined as being elastic or degenerate elastic if during the growth process the chemical driving energy is always in equilibrium with the resistive energy. The term degenerate elastic transformation refers to a process which shows small local discontinuities or jumps during the growth of a martensite plate. The transformation is said to be spontaneous or burst whenever the chemical driving energy exceeds the resistive energy to a great extent. Once the transformation starts, the growth or catalytic nucleation can not be suppressed by external influences.

2.2 PSEUDOELASTICITY

The pseudoelastic effect is a phenomenon by which a strain is attained through a stress-induced martensitic transformation (SIM) and such strain completely recoverable upon unloading due to reversible nature of the transformation. This behaviour can be described as a mechanical (as opposed to thermal) type of shape-memory. Figure 3 [6] shows an example of this behaviour in terms of a stress-strain curve for a Cu-Zn alloy. It has two plateau regions, an upper one

and a lower one. The upper plateau corresponds to formation of SIM, and the lower one corresponds to the reversion of the SIM. When the specimen is loaded martensite forms as a number of parallel plates which thicken and coalesce, eventually leading to a single crystal of martensite. The preferred martensite variant is that whose shape strain permits maximum specimen elongation in the direction of the tensile axis. Upon unloading the stress-strain relationship follows the lower plateau region, which involves the nucleation and growth of parellel plates of the parent phase. The plateau stresses depend upon the test temperature. The upper plateau stress is zero at the M_s temperature.

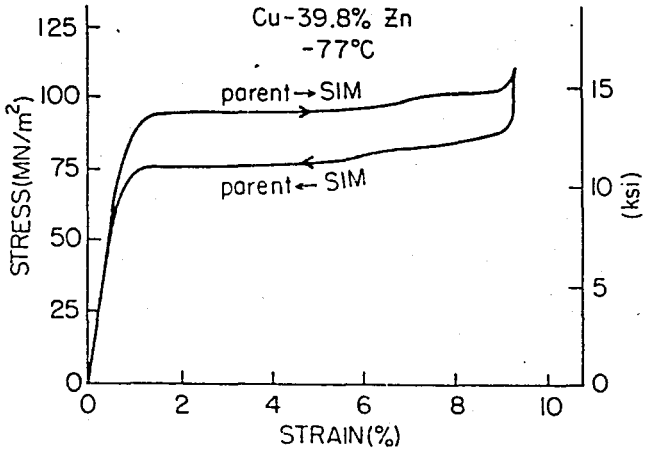

Figure 3 - Stress-strain curve for Cu-39.8 Zn (wt.pct.) alloy single crystal showing pseudoelastic loop due to formation and reversion of stress-induced martensite [6].

Figure 4 [6] shows the temperature dependence of the stress required to produce SIM. Because of the effective equivalence of temperature and stress with respect to thermoelastic martensitic transformations, σ^{P-M} decreases from a maximum near M_d to a minimum

near M_s. The parameter σ^{P-M} decreases with decreasing temperature because of decreasing stability of parent phase as M_s is approached. Similarly, the parameter σ^{M-P}, which is defined as the level to which stress must drop to allow the stress-induced martensite to revert to the parent phase, increases with increasing temperature from a minimum near A_s. This is because, the lower the temperature, the more stable is the martensite, so that the stress must be reduced to a greater extent to allow reversion to the parent phase. In fact, if the temperature is too low, no reversion at all will occur on unstressing the sample, i.e. no pseudoelastic behaviour will occur, and reversion to the parent phase will occur only on heating, i.e. only the shape-memory effect will occur. Although σ^{P-M} is greatly affected by temperature, it is not a strong function of strain, as seen in the Figures 3 and 4. The martensitic transformation temperatures in general are affected by stress [1]. For most shape-memory martensitic transformations the stability of the martensitic phase is enhanced by applied stress, so that the transformation temperatures M_s, M_f, A_s and A_f shift to higher values with increased stress.

In the left hand diagram of Figure 1(b) the stress-strain curve is drawn schematically whereas the diagram on the right in Figure 1(b) indicates the concomitant change in fractional martensite volume.

Many of the shape-memory alloys can undergo martensite-to-martensite transformations if sufficiently strained [3,7,17]. Both the normal martensite formed upon cooling and the SIM will undergo transformation. Figure 5 [17] shows the deformation behaviour of a Cu-39.8Zn (wt.pct.) alloy strained at -88°C, about 35°C above the M_s temperature. The first

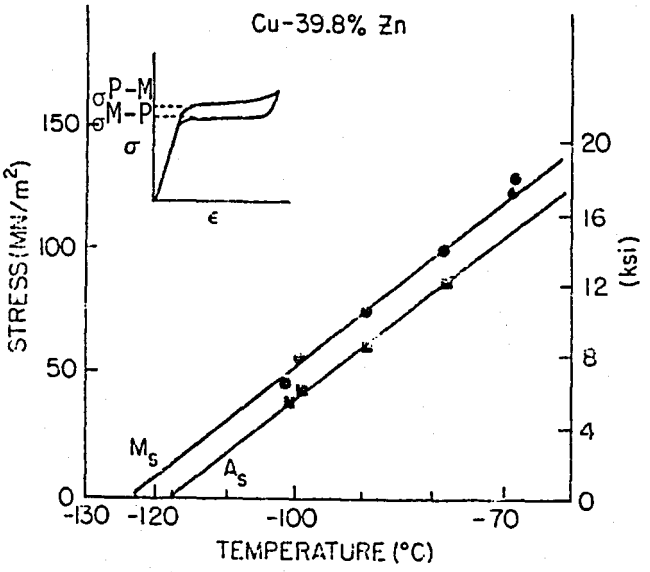

Figure 4 - Temperature dependence of the stress required to induce martensite in a Cu-39.8Zn(wt.pct.) single crystal [6].

upper plateu corresponds to the formation of SIM, as described above. However, the second plateau, which commences at about 9 pct. strain corresponds to a second martensitic transformation which is stress induced from the first martensite. The two lower plateaux results from the reverse transformations which occur in an inverse sequence. Taking advantage of these successive martensite-to-martensite transformations, completely recoverable strains as high as 17 pct. can be realized in Cu-Zn alloy.

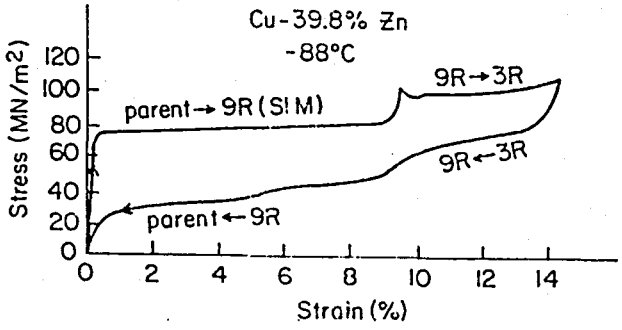

Figure 5 - Double pseudoelastic loop caused by a martensite-to-martensite transformation in a Cu-39.8Zn (wt.pct.) alloy. 9R and 3R correspond to different martensitic crystal structures [17].

2.3 SHAPE-MEMORY EFFECT (SME)

The shape-memory effect is one of the interesting properties associated with the martensitic transformation. The shape-memory effect consists of recovery, on heating, of the original (high temperature) shape of an alloy which has been apparently plastically deformed at low temperature. It must be noted that this phenomenon is irreversible. That is, the alloy remembers only the high temperature shape, and if cooled again to low temperature, will not further change shape. Figure 1(c) shows this behaviour schematically. The left-hand diagram shows the performance of a shape-memory experiment in a tensile test. The upper half represents the response of the specimen to the isothermal increase and decrease of the applied stress, the lower half to the effect of the subsequent temperature increase. The right hand diagram indicates

the change in fractional amount of martensite again. Figure 6 [2] shows crystallographic history of the spacecraft antenna as a function of temperature. The construction material, Nitinol wire in a large coil, is raised to a temperature of 650°C and is stabilized so that the crystal structure of the material is entirely in the beta, or "parent", phase (a). This phase is often the crystal structure austenite. The wire is now cooled. At the temperature M_s (60°C) the new crystal phase martensite starts to form, replacing the beta phase (b). At M_f (52°C) the transformation to martensite is finished (c). While the Nitinol wire is held at a temperature below M_f it is cut into short lengths, which are gently bent to form the segments of the intended hemisphere (d). Where the segments cross one another they are fastened by tack welding. One can now crush the antenna into a small volume (e). In order to restore the original shape the crushed structure is heated. At temperature A_s (71°C) austenite begins to replace martensite (f). On reaching A_f (77°C) the antenna has unfolded completely (g). In this particular case what the shape-memory alloy remembers, is not the actual configuration of the antenna but the gentle curves of the coiled wire from which the antenna was constructed. As the wire tries to straighten itself it is constrained to the shape of a bowl by the multiple welds at the crossover points.

On a microstructural scale what is happening when a shape-memory alloy is deformed and then unloaded and/or heated to recover its original shape is known reasonably [1]. First of all, the original (remembered) shape corresponds to the shape of the piece when the alloy was originally annealed in the range of the high temperature parent phase. When the

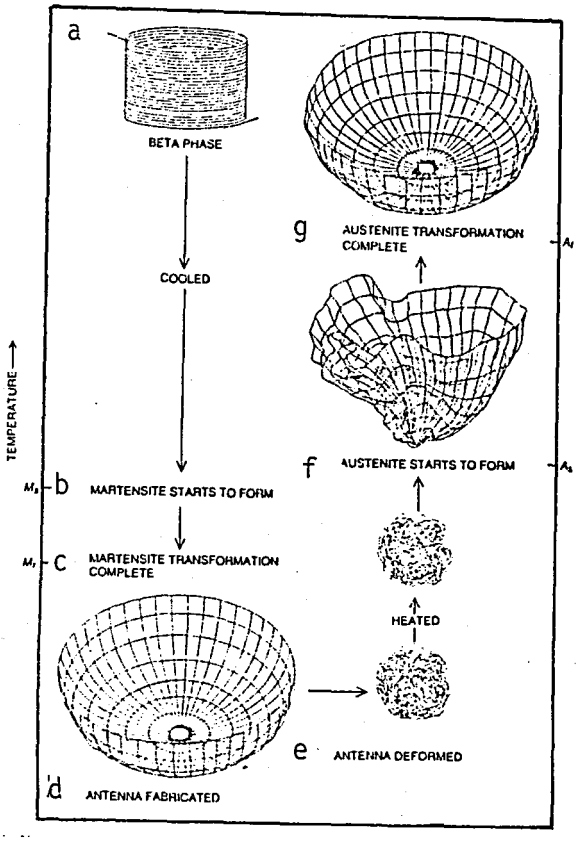

Figure 6 - Crystallographic history of the spacecraft antenna shows the role of temperature in the shape-memory effect [2].

alloy is subsequently cooled to lower temperatures, it will tend to transform spontaneously to the martensite phase or, if not cooled sufficiently, the high temperature phase will persist but in a metastable condition that is ripe for transformation to martensite under stress. Thus straining a shape-memory alloy corresponds either to deformation of martensite which may already be present or to formation of stress-induced martensite from the retained high temperature phase; or to both of these mechanisms. In any case, the subsequent shape

recovery is based on the fact that the strain introduced is in fact reversible, i.e. although it appears that there has been permanent plastic deformation (since recoverable strains of several percent may be realized, far beyond normal elastic limits) in fact there has been no permanent damage on a microstructural scale. The microstructure has deformed by mechanisms quite unlike the usual irreversible mechanisms of plastic deformation such as dislocation motion. Moreover, if the alloy is heated sufficiently that it prefers back to the high temperature phase, it does so because the deformations retreat along the exact path by which they were introduced, so that the original shape is recovered. One of the main reasons for the reversibility of thermoelastic martensite is that there are inherently low elastic strains associated with the crystal structure change, so that the elastic limit of the parent phase matrix is not exceeded and irreversible plastic deformation events do not occur. Furthermore, the strains which do build up as the martensite plates grow are effectively cancelled out by forming groups of mutually accommodating plates. In some cases these groups consist of simple alternating stacks of plates in which the strain vectors tend to cancelled between neighbouring plates; in other cases the plate groups are more complex. In addition, the individual plates themselves are internally twinned or faulted to accomodate the transformation strains. The reason that steels and many other martensitic alloys cannot exhibit shape-memory behaviour is simply that the transformations strains are too great to be accommodated in this way, so that irreversible events occur during transformation and thermoelastic behaviour is ruled out. When shape-memory alloys are deformed, they change their shape by shearing parent phase

regions to martensite, by detwinning within individual martensite plates (for internally twinned martensites) and by complementary growth and/or shrinkage of neighbouring martensite plates in groups.

In general, there is a complementary relationship between the shape-memory effect and pseudoelastic effect mentioned above. This is shown in Figure 7 [1]. At lower deformation temperatures a greater proportion of the initial strain is recovered by heating than by unloading, i.e. the shape-memory effect behaviour is more pronounced than the pseudoelastic effect. At higher temperatures the reverse is true.

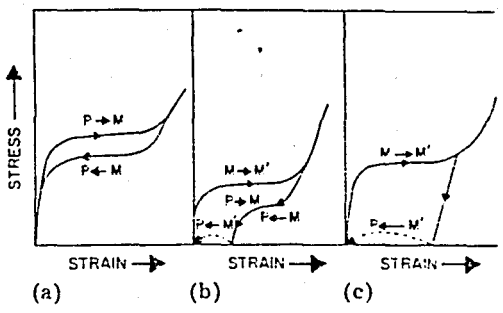

Figure 7 - Schematic stress-strain curves for a shape-memory alloy at various deformation temperatures T_d relative to the martensite transformation range, showing the complementary relationship of shape-memory effect and pseudoelastic effectbehaviour (P, parent phase; M, martensite; M', martensite formed by or altered by stressing; ____, loading and unloading; ---, heating): (a) $A_f < T_d = T_1 < M_d$; (b) $A_s < T_d = T_2 < A_f$ and M_d; (c) $T_d = T_3 < M_f$ [1].

2.4 TWO-WAY SHAPE-MEMORY EFFECT (TWSME)

As mentioned in the preceding part the term "shape-memory" means that the material remembers its pre-deformation shape, and reverts to this shape upon heating.

What then happens to the material geometry during subsequent cooling? Martensite must form if the material is cooled below its M_s temperature, but what may not be clear is whether it is the strained or the unstrained martensite which forms (i.e., the martensite structure and shape found prior to deformation, or that found after deformation). To understand this, one must examine exactly how the strain is being accommodated, or stored, in the material on a microscopic scale. In the as-quenched structure, the martensite plates are randomly oriented, and each individual plate is internally twinned in a random manner. When a load is applied, certain martensite variants and twin orientations are stabilized and begin to grow at the expense of others. Thus the material is able to store, or accommodate, strain by a combination of detwinning and reorientation mechanisms. Clearly there is a limit to the amount of strain that can be accommodated by such a process, and when this limit is approached, the slope of the stress-strain curve must begin to increase, until, finally, the dislocation yielding is observed. If the amount of deformation found in a material is less than that required for dislocation yielding, all of the strain stored in the material is recovered during heating, and randomly oriented and twinned martensite structure is again formed during cooling below M_f. There is a shape change during heating, but not during subsequent cooling,

as mentioned. This is called a "one-way shape-memory effect". Conversely, when the alloy is deformed by an amount sufficient to introduce or move dislocations, only part of the deformation can be returned during heating; the result is an imperfect one-way effect. In this case, however, a partial return to the deformed geometry is noted during subsequent cooling through M_s. This means that it is the deformed and reoriented martensite that is formed and not the original martensite structure; the presence of dislocations stabilizes the strained martensite structure. This is generally termed a "two-way shape-memory effect" (Figure 1(d)).

The training involved to produce the TWSME can be accomplished in two ways, or by combination of the two (Figure 8) [5].

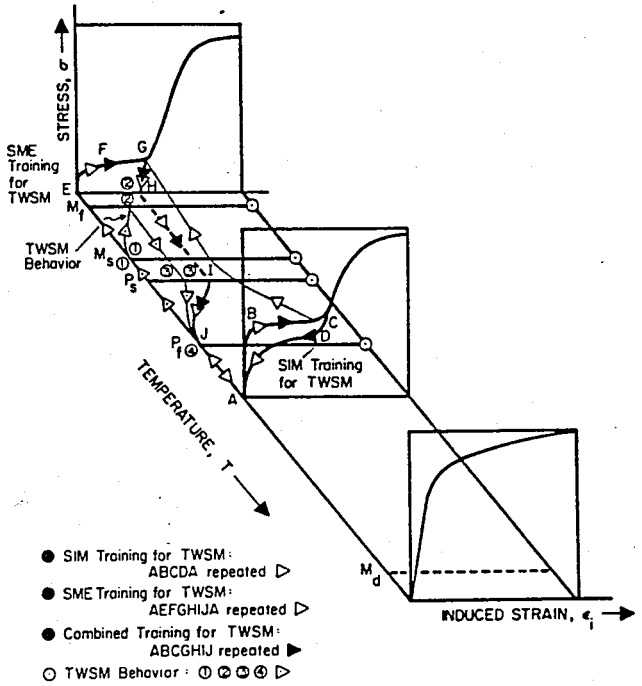

Figure 8 - Schematic illustration of training routines used to obtain 2-way shape-memory (TWSM) behaviour; SIM training for TWSM involves repeating the pattern ABCDA; SME training for TWSM involves repeating the pattern AEFGHIJA; "combined" training for TWSM involves repeating the pattern ABCGHIJA. After training the alloy will spontaneosly follow the TWSM behaviour pattern (1) (2) (3) (4) on cooling and heating [5].

a. The sample is strained in the martensitic condition, then heated above A_f and subsequently cooled below M_f; if the initial deformation is great enough and/or if the routine is repeated several times, the two-way memory will be exhibited on cooling, i.e. the sample will spontaneously move toward the initial low-temperature deformed shape on cooling. This is termed "SME training".

b. With the second method of TWSME training, the sample is repeatedly strained above A_f, thus creating and reverting from stress-induced martensite via pseudoelastic effect; the two-way shape-memory is exhibited on cooling below M_f. This is termed "SIM training".

c. In a combination of the above routines (combined training), the sample is strained pseudoelastically above A_f and then cooled below M_f while maintaining the strain in the sample; the sample is then unloaded and heated above A_f; if this routine is repeated several times, the two-way shape-memory behaviour is exhibited.

Figure 9 [18] shows the micrograph of a specimen which underwent on SME training and was then cooled to M_f. The A-D, variants with nearly the same shape strains are dominant (a). Further loading shows that D variant is the preferred variant (b) after a strain of 5 pct (Cu-39.8Zn (wt.pct.) alloy).

Schematic examples of the TWSME are shown in Figure 10 [17].

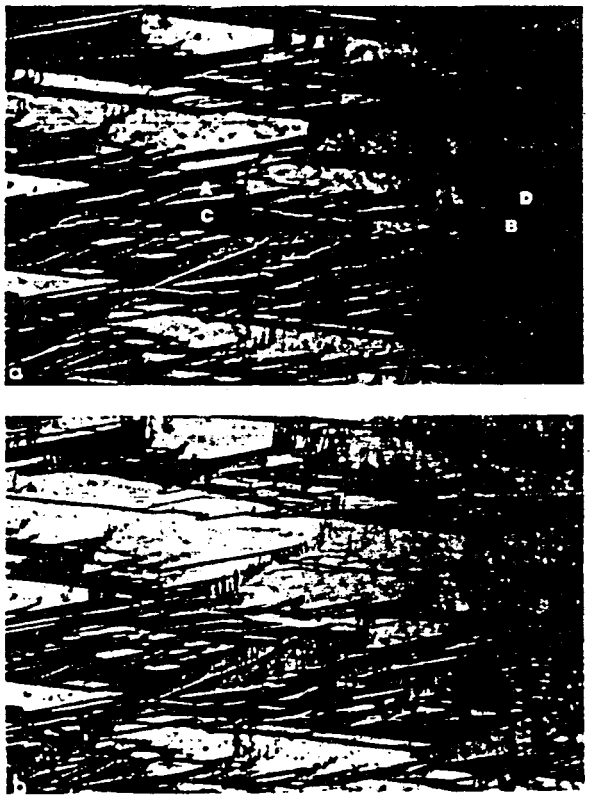

Figure 9 - Optical micrographs showing the two way SME.

a) corresponds to the initial martensite structure.
b) corresponds to the second cycle on cooling after deforming (a) below M_f. Note the predominance of the D variant in (b) [18].

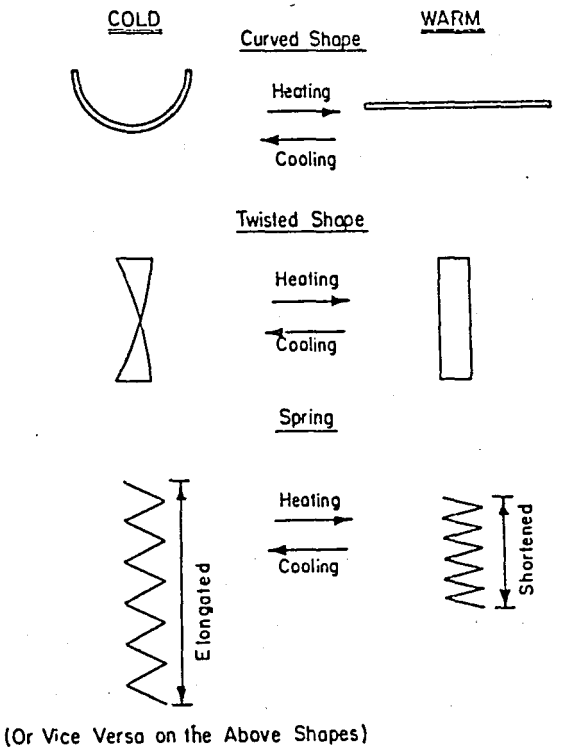

Figure 10 - Schematic showing various examples of the two-way shape memory effect [17].

2.5 SHAPE-MEMORY MECHANISM IN ALLOYS

Substantial progress has recently been made in understanding the nature of SME. The four stages which involve the effect are schematically illustrated in Figure 11 [17,19].

On cooling, a crystal of parent phase will transform into many orientations of martensite. In all cases, six groups of four variants form from the parent, and the average shape strain in each group becomes nearly zero. Thus, the initial length L of the material does not change.

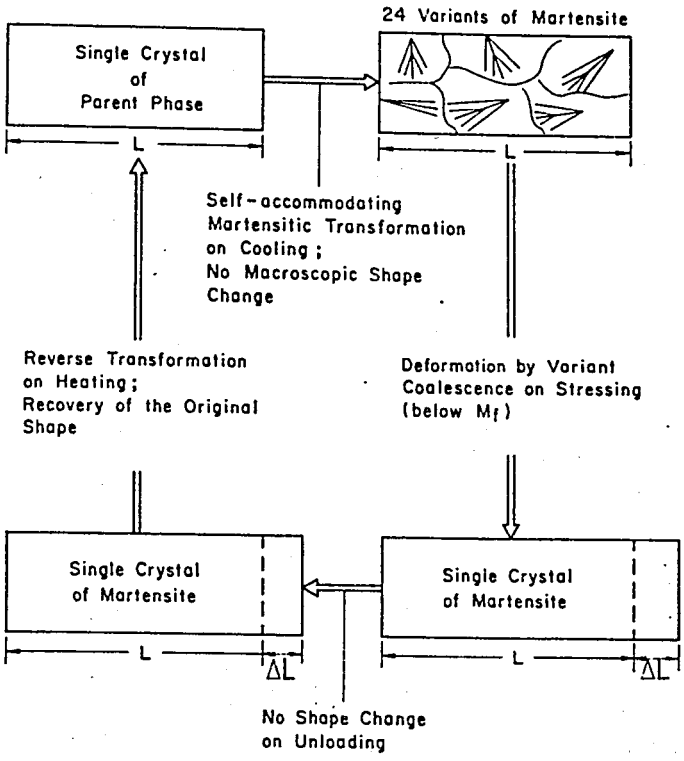

Figure 11 - Schematic showing various processes involved in the shape-memory effect [17,19].

When this multi-orientation configuration of martensite is deformed, a single orientation of martensite eventually results because of twinning and the movement of certain martensite interfaces. The end result is a single crystal of martensite with the particular correspondance whose shape strain involves the maximum extension in the direction of the applied stress. By this process the specimen is elongated from L to L + ΔL.

On releasing the applied stress, the elongation (ΔL) remains since the reverse rearrangement of twins and variants does not occur.

On heating the single crystal of martensite, the reverse transformation to the parent phase takes place and the original length L is again assumed.

This sequence is metallographically depicted in Figure 12 [8,17].

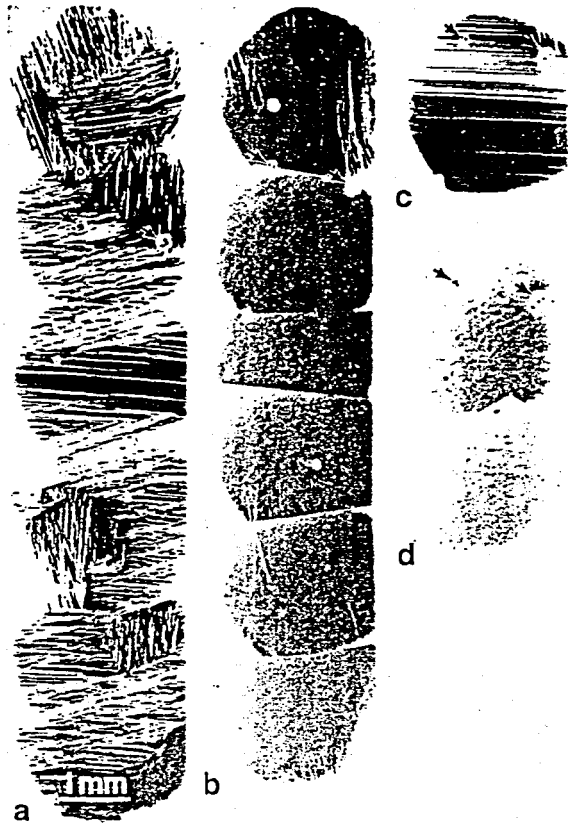

Figure 12 - Optical micrographs showing (a) numerous orientatations of martensite in as-transformed Cu-Zn-Ga alloy, (b) the "coalescence" of variants upon stressing, (c) nucleation of only a single variant of the parent phase during heating, and (d) the original single crystal of the parent phase [8,17].

2.6 APPLICATIONS OF SHAPE-MEMORY BEHAVIOUR

Potential engineering application of SME alloys is increased in recent years. Applications have taken clever advantage of two main parameters: the shape change on heating through a certain temperature

range and the internal stress developed if this reverse transformation is opposed (such as by physically blocking the movement or adding an external load).

Wayman [8] classifies the uses of shape-memory alloys as industrial, energy, and dental/medical categories. Most applications involve Ni-Ti type and Cu-based alloys, the latter being relatively inexpensive to produce and fabricate into numerous forms.

2.6.1 Industrial Applications

a) Fasteners and Couplings

One of the earliest widespread applications of SME is Raychem Corporation's (Menlo Park, Calif.) introduction of tubing or pipe couplings which shrink during heating. Typical type of such Ni-Ti type couplings are those used for connecting aircraft hydraulic lines. The couplings are expanded ~4 pct. in the martensitic condition at liquid-nitrogen temperature, then placed around the tubes to be joined. During warming to room temperature, they contract, producing a tight seal. Figure 13 [2] shows hydraulic-tube couplings for the Grumman F-14 jet fighter fabricated from a Nitinol alloy. It has a martensite-formation temperature, M_s, in the cryogenic region below -120°C. The sleevelike coupling is machined at normal temperature to have an inner diameter 4 pct. less than the outer diameter of the tubes to be joined. The sleeve is then cooled below the M_s temperature and is mechanically expanded to have an inner diameter 4 pct. greater than the tubes' outer diameter (top). Still held at a temperature below M_s, the sleeve is

placed around the ends of the tubes. When the coupling is warmed, it shrinks to form a tight seal (bottom). Ribs machined into the sleeve enhance seal by biting into tubes. The use of such fittings avoids metallurgical degradation which can result from welding or brazing, and avoids damage to aircraft skin.

Raychem recently introduced a new line of Cu-based alloy heat - shrinkable fittings in addition to other fasteners and devices. Figure 14 [8] is photograph of a clamp made of a Cu-based SME alloy.

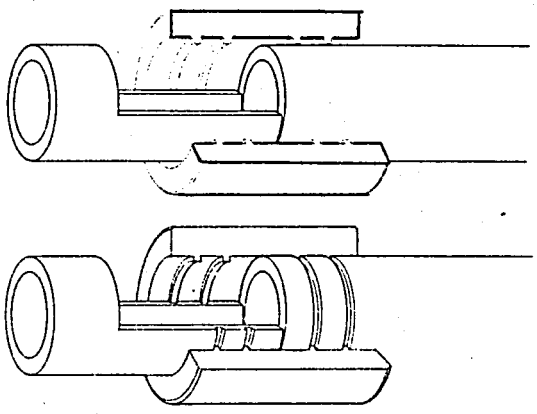

Figure 13 - Hydraulic-tube couplings for the Grumman F-14 jet fighter fabricated from a Nitinol alloy [2].

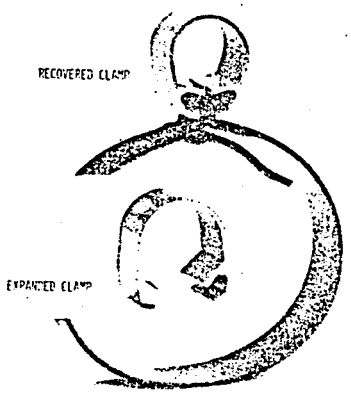

Figure 14 - Clamp made from Cu-based shape-memory alloy (Courtesy Raychem Corp.) [8].

b) Thermomechanical and Thermostatic Devices

Substantial efforts in developing Cu-based shape-memory alloys have been made by the Delta Memory Metal Company (Suffolk, England). They have developed a range of Cu-Zn-Al SME alloys with emphasis on thermostats, controls for heating and cooling equipment, automative control devices, and actuators for equipment ranging from green house

windows to fire doors. Many of these prototypes have been cycled a half-million times or so with no observable fatigue, creep or change in deflection characteristics.

Figure 15 [2] shows an actuator for green house windows, basically a spring-loaded hinge containing a bias spring and a SME spring. At temperatures below about 18°C the spring is fully contracted and the window remains closed. When the temperature rises above 18°C, shape-memory spring overcomes the force of bias spring and begins to open the window. At 25°C the actuating spring is fully extended. The window is automatically pulled shut when the temperature falls.

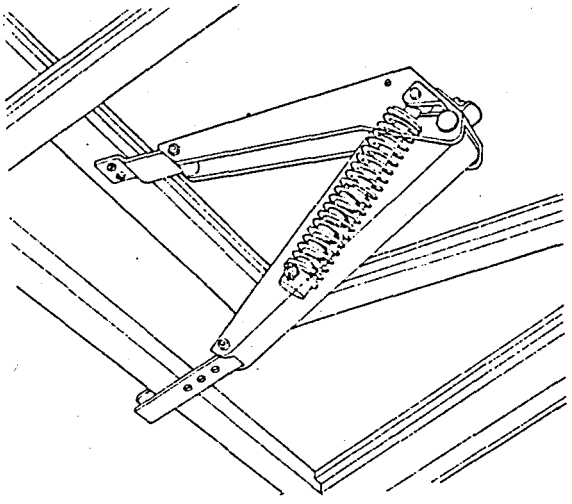

Figure 15 - Simple window opener that would be suitable for a green house is actuated by a spring fabricated out of a copper-rich shape-memory alloy [2].

c) Recording Pen Drive Unit

The Foxboro Company (Foxboro, Mass.) has developed a pen drive that exploits the shape-memory response of Nitinol wire. The servo-drive unit (Figure 16 [20]) contains a Ni-Ti wire maintained under

tensile stress. The input signal is converted to a current which is induced into the SME wire, the thus heated wire changes its length and moves a connected lever. This device eliminates many moving parts and is extremely reliable.

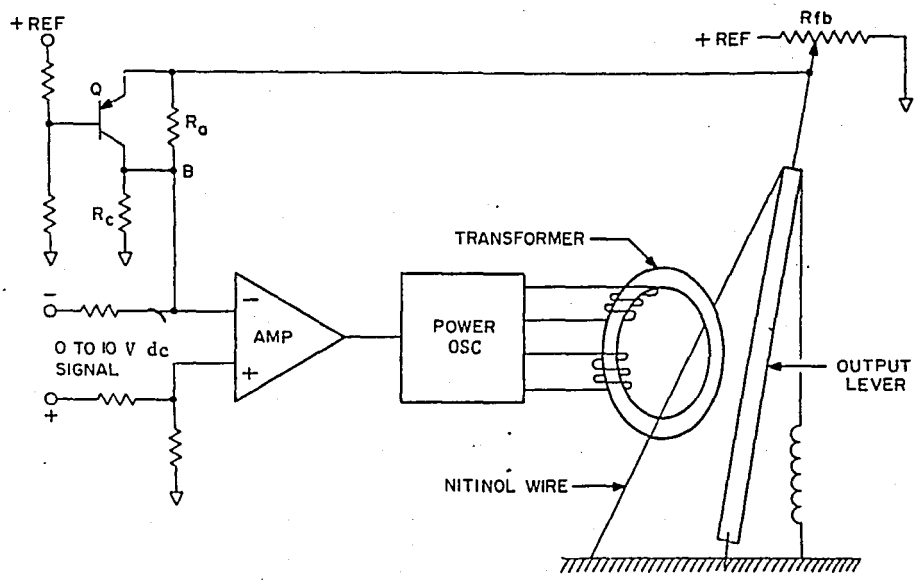

Figure 16 - Simplified drawing of drive unit [20].

2.6.2 Energy Applications

Large stresses are generated during the shape-memory effect. For example, in Ni-Ti alloys stresses as high as 100 000 psi are created by the reverse transformation of the deformed martensite to the memory configuration during heating. Such stresses are an order of magnitude higher than those necessary to deform the martensite at lower temperature. Thus, heat can be used to create a mechanical force which can do work.

The principle of Nitinol heat engine operation is illustrated in Figure 17 [21]. In Figure 17(A), a Nitinol element is shown at

temperature $T_1 < M_f$. In Figure 17(B), a weight W_1 is applied and work is done on the Nitinol element, $W_1 d_1$, where d_1 is the deflection. In Figure 17(C), a second weight, W_2, is added at constant d_1 and T_1. In Figure 17(D), the Nitinol element temperature is raised to $T_2 > A_f$ and the work performed by the Nitinol is $(W_1 + W_2)d_1$. The net work performed during the operations is $W_2 d_1$.

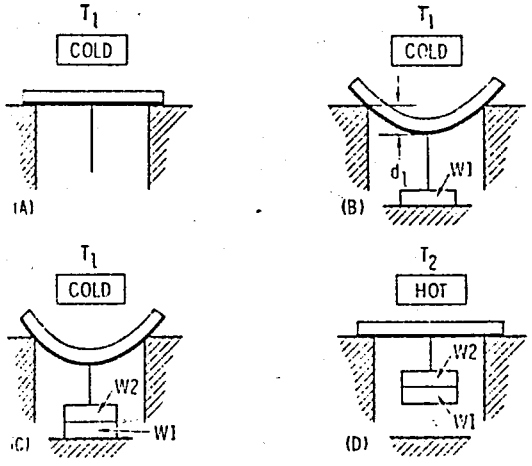

Figure 17 - Conceptual cycle of Nitinol thermal-to-mechanical energy converter (after Buehler and Goldstein) (A) Nitinol element memory form; (B) element deformed by weight W_1 at T_1; (C) element subjected to total weight W_1+W_2 at T_1; (D) element restored to original form at T_2 loaded with weight W_1+W_2 [21].

2.6.3 Dental and Medical Applications

There have been some interesting dental and medical applications, including teeth braces, orthopedic bone-straightening and fracture-aligning devices, blood clot filters, intracranial aneurism clips, prosthetic muscles for an artificial heart and intrauterine contraceptive devices [8,22-24].

III. Cu-Al-Ni ALLOY SYSTEM

Superelasticity and shape-memory effect in Cu-Al-Ni alloys in the composition range 14 to 14.5 Al and 2 to 4.4 Ni (wt.pct.) have been extensively studied by some workers [7,9,10,25-29].

The high temperature β_1 phase in Cu-Al-Ni alloys can be retained at room temperature by rapid quenching. The alloy is extremely unstable in the quenched state and undergoes a martensitic transformation on further cooling or by application of stress above M_s. In the latter case, strain is accomodated by formation of the martensite and pseudoelastic behaviour occurs if the strain is recovered by reversal of the transformation during removal of the stress. On the other hand, if the martensite stable on removal of stress, the strain may be recovered by reverse transformation during subsequent heating and then one kind of shape-memory behaviour is evident. A more usual kind of shape-memory behaviour is associated with deformation of a martensitic structure and recovery of the strain during reverse transformation on heating. For appropriate alloys in the system Cu-Al-Ni pseudoelastic behaviour occurs at temperatures above A_s, and shape-memory effect at temperatures near and below M_s [28].

Cu-Al-Ni alloy system undergoes a martensitic transformation to either the γ_1' or the β_1', depending on the exact composition of the alloy [4]. Stressing of alloys results in the formation of four different martensitic products; β_1', β_1'', γ_1' and α_1' [4,7].

It is also interesting to note that the M_s temperature is very sensitive to the alloy composition. A very small change in composition would change the M_s temperature very much. Thus the martensitic transformation can be completely missed if the alloy composition is not carefully controlled.

Rachinger and Busch et al. [28] have obtained very large elastic strains in single crystal specimens of 82.5 Cu-14.5 Al-3 Ni (wt. pct.) with M_s~-10°C. They obtained best results when the single crystals oil quenched from the β phase region. Rachinger obtained elastic strains of 4 pct. at room temperature using a 3-point bending method, whilst Busch et al. obtained elastic strains of up to 24 pct. in tensile and compressive loading of both the β_1 and the low temperature martensitic structure. Busch also observed that superelastic behaviour could be observed in coarse grain polycrystalline specimens.

Cu-Al-Ni alloys are inherently quite brittle. For example, when Cu-14.2 Al-3.3 Ni (wt. pct.) is cast, it has a room temperature tensile ductility of only 0.6pct. Table III [4] shows some properties of the same alloy.

TABLE III - Properties of Cu-14.2 Al-3.3Ni [4]

Grain Size	1500 μm
Ultimate tensile strength	440 MPa
Yield strength	360 MPa
Ductility	0.6 pct.

3.1 PHYSICAL METALLURGY AND PHASE DIAGRAMS OF THE Cu-Al-Ni ALLOY SYSTEM

The Cu-Al-Ni system is metallurgically quite complex. Figure 18 [30] shows the equilibrium phase diagram for a binary Cu-Al alloy superimposed with a metastable phase diagram. The shape-memory alloy Cu-Al-Ni, having a composition near that of Cu_3Al, exhibits an order disorder transformation from the disordered bcc β phase to the ordered fcc β_1 phase at high temperature. The β_1 phase has the DO_3 structure with aluminium atoms at the face center and corner positions, and Cu and Ni atoms at the edge and interior points. Although the β_1 phase is a nonequilibrium phase, it nonetheless remains stable at room temperature upon quenching from the high temperature β phase. If the alloy is slowly cooled from the austenitic phase (β_1), $\alpha + \gamma_2$ eutectic will form. If, on the other hand, the alloy is rapidly quenched through the M_s temperature, the parent DO_3 phase undergoes a martensitic transformation to either the γ_1' or the β_1' structure, depending upon the Al content [4,30]. It is well established that Cu-Al-Ni alloys with the composition around Cu-14.2 Al-4.3 Ni (wt.pct.) transform from the β_1 phase to the γ_1' phase when cooled below M_s temperature [31]. The γ_1' martensite usually appear in spear-like form (polycrystals) or in thick bands (single crystals), and internal twins are invariably present in the martensite as the lattice invariant strain [16,25,31].

K. Otsuka et al. [25] found that the structure of the martensites stress-induced above M_s is temperature dependent. That is, if the temperature is higher than A_f, the β_1' martensite is stress induced, while

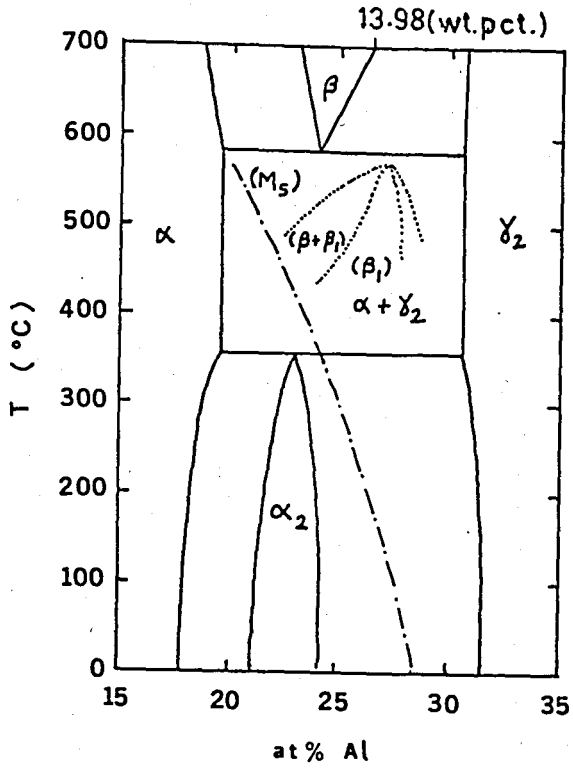

Figure 18 - The phase diagram for Cu-Al alloy [30].

_____: equilibrium phase
.....: metastable DO_3 phase
_.-._.-._: martensite phase

the temperature is lower than A_f, the γ_1' martensite is stress-induced, which has the same crystal structure as that of the thermally formed martensites. The β_1' martensite has a acicular (thin plate) structure, and the lattice invariant strains of the martensite are stacking faults on the basal plane [25,28]. K. Otusuka et al. [26] further found successive transformations from the stress-induced β_1' to α_1', and have shown that all the structures of the stress-induced martensites are kinds of long-period stacking order structures with the common basal plane, their difference lying solely in their stacking sequence. This means that to transform one structure to another, only a rearrangement

in the stacking sequence is involved. It was confirmed recently that the martensite stress-induced from γ_1' is different from the β_1' stress induced from β_1. It is called β_1'' [7]. K. Otsuka et al. [7-26] proposed a schematic phase diagram (Figure 19 [7]) relating the phases β_1, γ_1', β_1', β_1'' and α_1' in temperature stress coordinates. Here two diagrams are drawn by broken lines and full lines. The former is the one which K. Otsuka et al. [26] proposed some years ago, while the latter is the one K. Otsuka et al. [7] recently deduced. In phase field O_1CDO_2, β_1' is a stable phase, while β_1'' a metastable one. Anyway β_1'' is always stress-induced from γ_1', while β_1' is stress-induced from β_1. Both transform into α_1' by further loading, but α_1' transforms back to β_1' irrespective of whether it has been transformed from β_1'' or β_1', indicating that β_1' is stabler than β_1''. The reason why β_1'' is stress-induced from γ_1' in spite of its metastability is that the mechanism of the $\gamma_1' \rightarrow \beta_1''$ transformation is more favorable than that of the $\gamma_1' \rightarrow \beta_1'$ transformation under an uniaxially stressed condition. The β_1' phase in the phase field O_2EFG is also a metastable phase, which appears due to the lack of direct transformation mechanism between β_1 and α_1'.

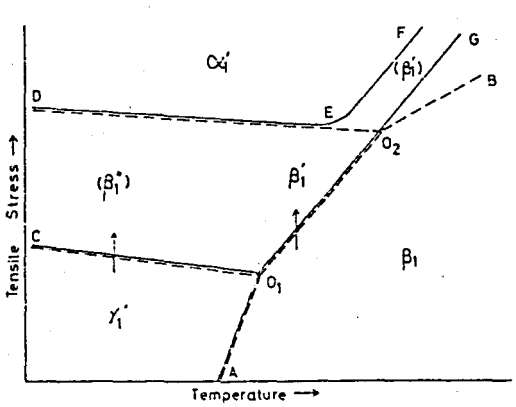

Figure 19 - Schematic phase diagram of a Cu-Al-Ni alloy [7].

Since the specimens used in this study produced essentially γ_1' martensite, only γ_1' martensite will be treated in the following.

3.2 MORPHOLOGY OF THERMOELASTIC γ_1' Cu-Al-Ni MARTENSITE

A typical thermoelastic martensite has a "spear like" form consisting of two parts divided by a ridge at the center as shown in Figure 20 [31] which was taken from a bulk specimen. It was heat-treated at 1000°C for 1 hour and then quenched into water at 100°C.

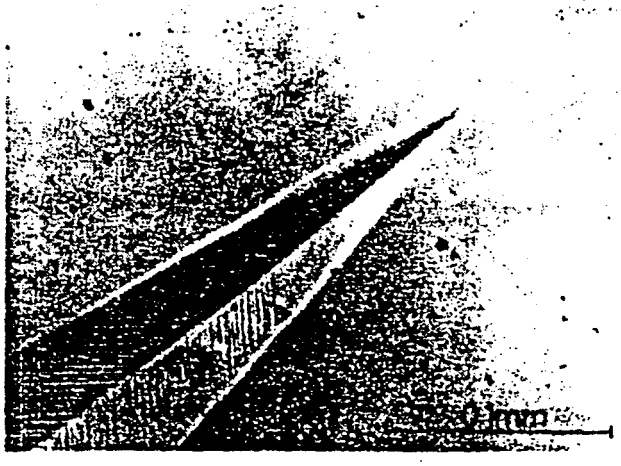

Figure 20 - Optical micrograph of a typical γ_1' Cu-14.2Al-4.3Ni (wt.pct.) martensite. Unetched [31].

It is quite large. Figure 21(a) [31] also shows small γ_1' martensites observed in specimens which were heat-treated at 1000°C for 1 hour and then quenched into water at 20°C. The martensites in Figure 21(a) are similar to those in Figure 20 in morphology except in their dimension. Figure 21(b) shows a diffraction pattern taken from the area framed with dotted lines in Figure 21(a). The pattern consists of two sets of

reflections which are twin-related to each other with the (121) γ_1' twinning plane. Trace analysis shows that the (121) γ_1' twinning plane coincides with the plane of ridge between the two halves (I and II in Figure 21(a)). Thus it is concluded that the two halves are twin-related to each other with the (121) γ_1' twinning plane as a plane of ridge. The streaks in two directions observed in the diffraction pattern (Figure 21(b)) are exactly normal to the basal plane of each martensite (I and II) and also to the striations (↑) in the micrograph (a). Thus these streaks are identified as due to stacking faults on the basal plane. Figure 21(c) is a diffraction pattern taken from the area framed with solid lines in Figure 21(a). Figure 21(a) also shows the habit planes between matrix β_1 and martensite γ_1' determined by the trace analysis.

Figure 22 [31] shows a clear picture of "spear like" martensite in bulk on a microscopic scale. Although two halves on both sides of ridge can be regarded as variants of martensite as well as twins to each other, internal twins can not be regarded as variants of martensite with respect to the matrix. γ_1' martensites in bulk have two kinds of defects, internal twins and stacking faults. Internal twins within each variant are considered to be lattice invariant strain, and the stacking faults on the basal plane in each internal twin are considered to be due to accidental stacking error upon transformation.

Why does a spear-like martensite consist of two twin related halves divided by a ridge? The answer may be given by assuming that "spear like" shape minimizes the strain energy set up around the interfaces between the matrix and martensite. Habit planes of martensite have specific indices (i.e., $\{331\}_{\beta_1}$) on account of the conformity of the lattices of

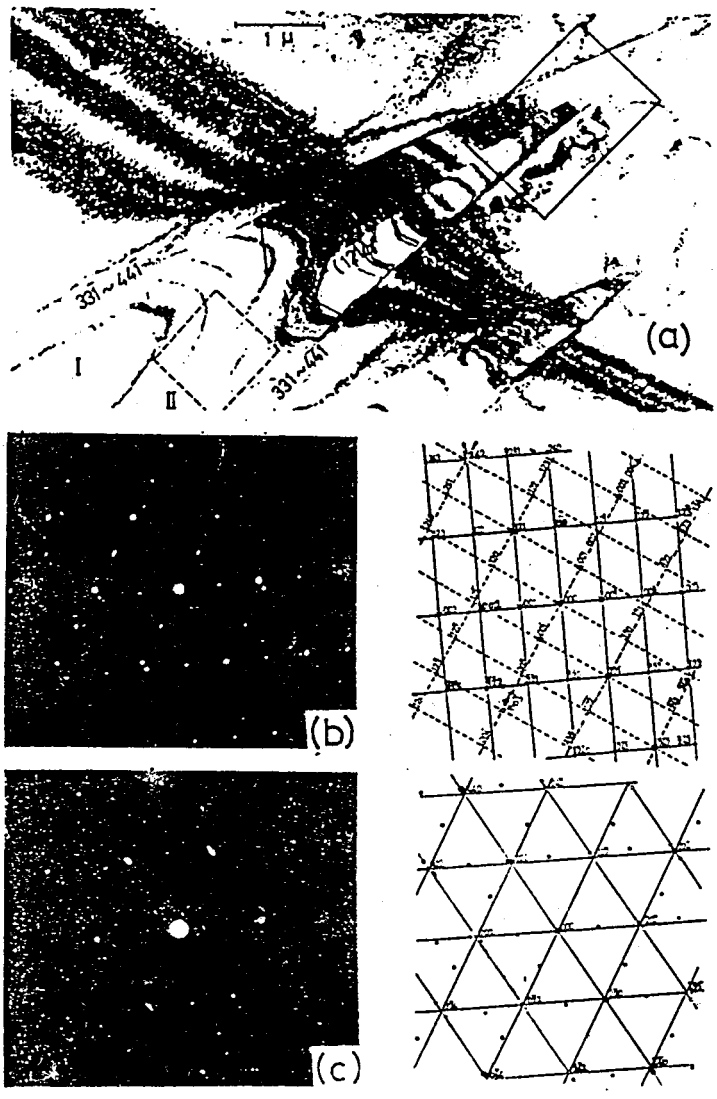

Figure 21 - (a) Electron micrograph of a "small" martensite. (b) Diffraction pattern taken from the framed (with dotted lines) area in (a), showing that martensites (I) and (II) are twin related with $(121)_{\gamma}$ as a twinning plane. Marks • and ○ in the key diagram represent fundamental reflections from (I) and (II), respectively. Marks ⊙ and ⊙ represent reflections due to double diffraction. Striations in (a) (↕) and streaks in (b) are normal to each other. (c) Diffraction pattern taken from the framed (with solid line) area, showing orientation relationship. Only matrix reflections, which are located by the cross point of three straight lines, are indexed, since martensite reflections are the same as those in (b) [31].

martensite and matrix or on account of the invariance of habit plane required in the phenomenological theory of martensite. Twin related "spear like" martensites divided by a ridge can satisfy both the energy condition and the conformity condition stated above, the energy produced by the creation of boundary being small since the twin boundary is coherent.

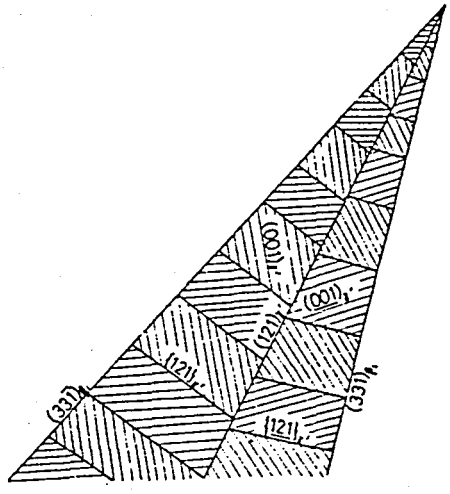

Figure 22 - Diagrammatical illustration of the morphology of a γ_1' "spear-like" martensite in bulk specimens [31].

3.3 CRYSTAL STRUCTURES OF MARTENSITES

The crystal structures of all the martensites are found to be kinds of long-period stacking order structures, with the common basal plane shown in Figure 23(a) [7], and the stacking sequence of each structure is shown in Figure 23(b)-(e). More detailed information on the crystal structures is summarized in Table IV [7].

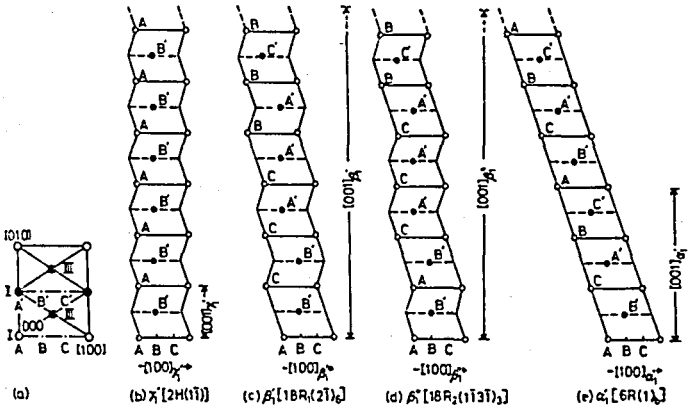

Figure 23 - Crystal structures of various stress-induced martensites (a) represents the atomic arrangement and possible stacking sites in the common basal plane. Open circles represent Al atoms and closed ones Cu (and extra Ni and Al) atoms. (b)-(e) represent stacking sequence of each structure, viewed from $[010]_{\beta_1'} = [010]_{\beta_1''}$ etc. directions [7].

TABLE IV - Crystal Structures of the Various Stress-induced Martensites [7].

Phase	γ_1'	β_1'	β_1''	α_1'
Ramsdel notation	2H	$18R_1$	$18R_2$	6R
Stacking sequence	AB'	AB'CB'CA' CA'BA'BC' BC'AC'AB'	AB'AB'CA' CA'CA'BC' BC'BC'AB'	AB'CA'BC'

3.4 STRESS-STRAIN CURVES AS A FUNCTION OF TEMPERATURE

3.4.1 Single Crystal Specimens

Typical stress-strain curves as a function of temperature are shown in Figure 24 [16]. Otsuka et al. [16] divided these curves into three temperature regions according to the characteristics of the stress-strain curves.

In range (I) ($T > A_f$) the curves are characterized by an extremely small hysteresis, no peak at the yield points and general smoothness although serrations are still present on a microscopic scale. Yielding after linear elastic deformation upon loading corresponds to the stress-induced martensitic transformation, and the disappearance of strain upon unloading is due to the reversible reverse transformation. Thus, the curves in this temperature range (a) and (b) represent a pseudoelasticity effect.

In range (II) ($A_f \geq T > M_s$) the curves are characterized by a sharp peak at the yield point and a large hysteresis or a large residual strain (which is recoverable by heating, i.e. the shape-memory effect). The yielding after linear elastic deformation corresponds to a stress-induced martensitic transformation, and the closed curve at temperatures near A_f (d) represents a pseudoelastic loop.

The curves in the third temperature range ($T < M_s$) are characterized by the absence of linear elastic deformation. In this range martensites are present from the start. Thus, mobile lattice defects such as boundaries between martensite and the matrix or internal twins are present which cause plastic deformation even at very low stress levels and eliminates

the elastic deformation region. This temperature range is directly related to the shape-memory effect.

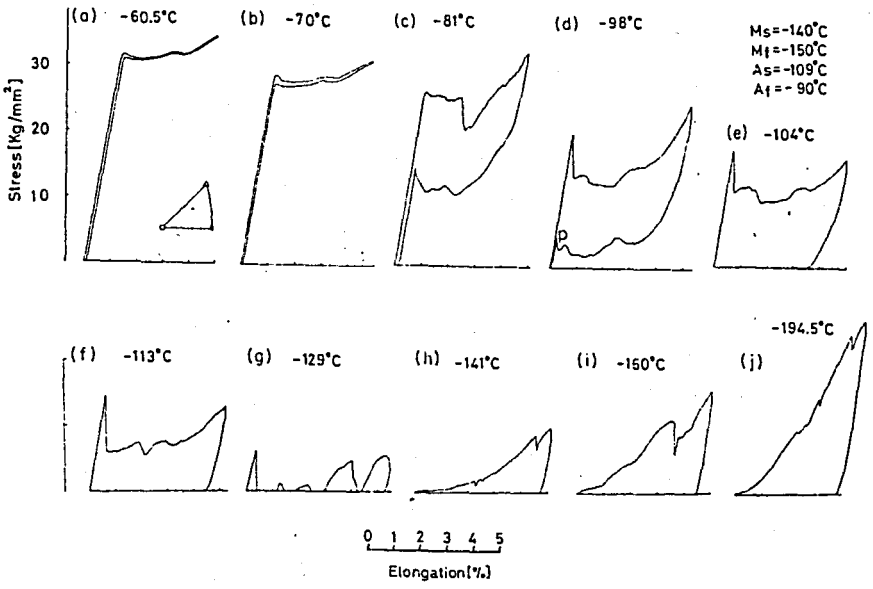

Figure 24 - Stress-strain curve as a function of temperature for Cu-14.5 Al-4.4 Ni (wt. pct.) single crystal. Maximum strain is restricted up to 5% in each curve. Strain rate 2.5 x 10^{-3}/min [16].

Typical morphological changes during a tensile test in the range $T > A_f$ are shown in the series of macrographs of Figure 25 [16] along with the corresponding stress-strain curve. In Figure 25,(a-g) correspond to the loading process, and (a'-g') correspond to unloading. Upon loading, starting from the single crystal state in the β_1 matrix phase (a), no structural change occurs in the linear elastic range until point b is reached in the s-s curve, where a few martensite plates appear (lower right corner b). With increasing strain more and more plates are

nucleated and some of them coalesce into thicker plates. Eventually at point e the specimen becomes essentially a single crystal. Thus the elongation between b and e (≈ 7.2 pct.) corresponds to that obtained from the shape strain of the stress-induced transformation. With further increase of stress no structural change is observable, and the curve between f and g is almost linear. Upon unloading from point g no structural change occurs until point a' is reached, and at point b' thin plate matrix regions are nucleated in the martensite. With decreasing strains more and more matrix regions are nucleated. Eventually at point g' the specimen reverts to the original β_1 matrix.

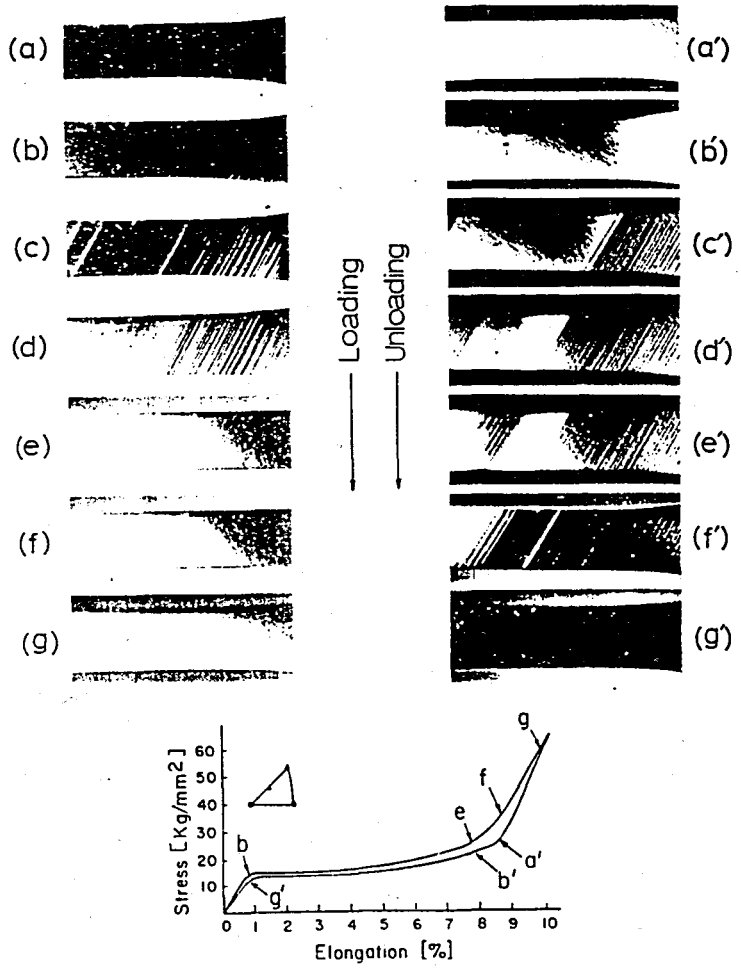

Figure 25 - Macroscopic morphological change associated with the $\beta_1 \rightleftarrows \beta_1'$ transformation at 27°C for Cu-14.1Al-4.2Ni (wt.pct.) single crystal (a) to (g) correspond to loading, and (a') to (g') correspond to the unloading process [16].

3.4.2 Polycrystalline Specimens

Stress-strain curves for the Cu-14 Al-3 Ni (wt. pct.) specimens are shown in Figure 26 [28]. These curves are significantly different from those for single crystals specimens, but Oishi and Brown [28] still divided them into temperature ranges relative to M_s, M_f, A_s and A_f.

Below M_f, Figure 26(a), the stress-strain curve is that characteristic of a ductile material and there is a large permanent set on removal of the stress.

Between M_f and A_s, Figure 26 (b), SIM is formed above a critical stress and serrations suddenly appear in the curve above this value of the stress. The serrations are much smaller than with single crystal specimens and there is no great decrease in stress level when SIM forms. The reason for this difference is that in single crystals, bands of SIM form right across the specimen giving a large elongation, whilst in polycrystalline specimens the SIM will form essentially in only one grain thus causing only a small portion of the cross section to elongate.

Above A_s fairly high stresses are required to nucleate SIM. In this temperature range, the stress-strain curve shows two linear portions, Figure 26 (c), the second corresponding to formation of SIM. The SIM formed in this temperature range should be unstable at zero stress, and indeed there is a considerable recovery in length on removal of the stress. There is always some permanent set remaining in the specimen, however, due presumably to plastic deformation and residual tensile stresses in the matrix.

At high temperatures (>10°C above A_f), SIM does not form at stresses less than the tensile strength of the material (5×10^4 psi) and the

specimen thus has a linear tensile curve with a maximum elongation of only 1 pct. at fracture.

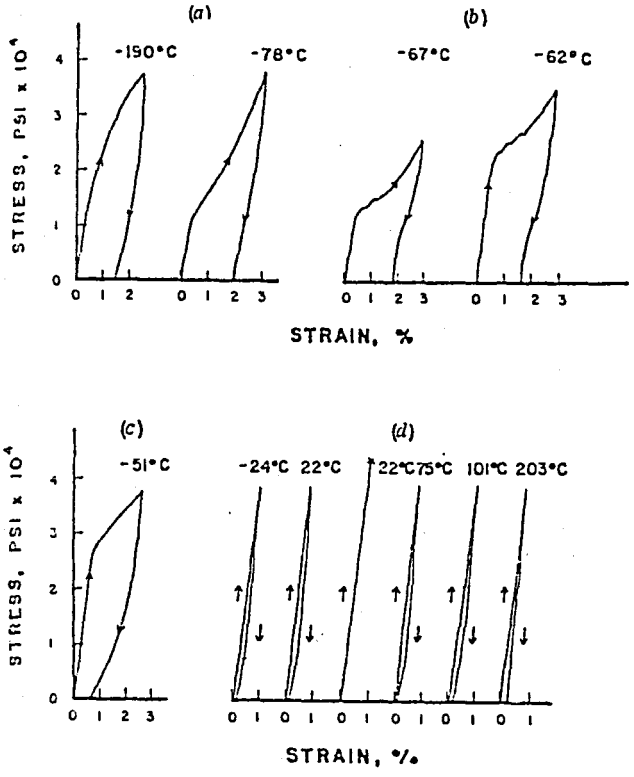

Figure 26 - Effect of temperature on the tensile behaviour of Cu-14 Al-3 Ni (wt.pct.) polycrystalline specimens. (a), (b), (c), (d) refer to different temperature ranges [28].

Figure 27 [28] shows the microstructure obtained on deforming a Cu-14 Al-2 Ni (wt.pct.) alloy at room temperature. The stress-strain curve for this specimen is very similar to that in Figure 26 (c). In the initial linear portion of the curve, platelike thermoelastic martensite forms. This is always reversible on removal of the stress. At higher stresses the burst martensite suddenly forms, Figure 27 (b), corresponding to the region in the tensile curve in which serrations appear. With increasing stress, Figure 27 (c), the regions of burst-type

martensite in a given grain expand and other areas of burst martensite nucleate in other grains. Even at fracture, however, transformation to the martensite is not complete owing presumably to the constraines by the grain boundaries.

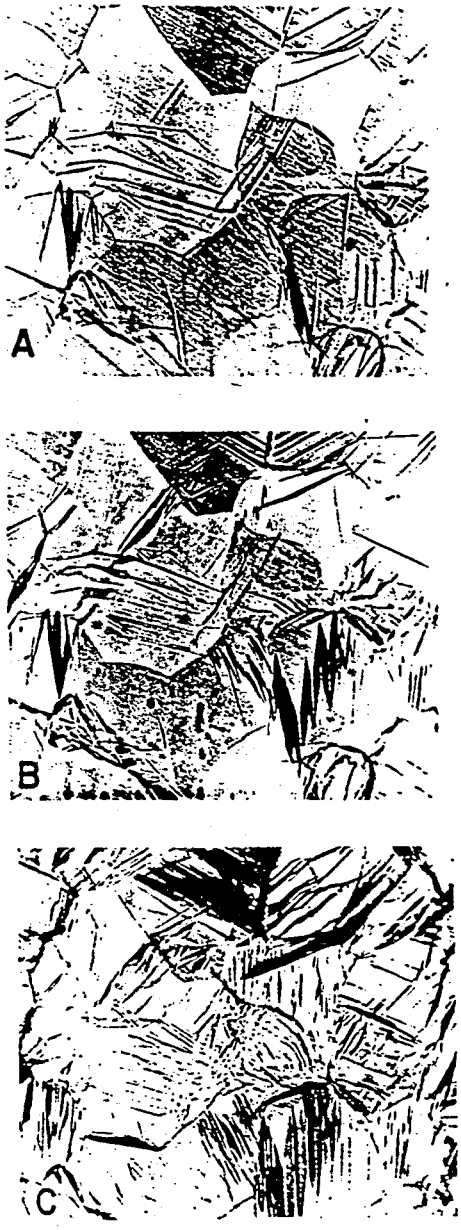

Figure 27 - Observations of the microstructures observed on progressively deforming a Cu-14 Al-2 Ni (wt.pct.) polycrystalline specimen [28].

Table V shows two compositions of polycrystalline material with the transition temperatures mentioned above.

TABLE V - Compositions and M_f, M_s, A_s and A_f Temperatures of Polycrystalline Material [28].

Nominal Composition	Chemical Analysis			M_f	M_s	A_s	A_f
	Cu	Al	Ni	°C			
Cu-14Al-2Ni	83.85 70.55	13.75 27.30	2.37(wt.pct) 2.16(at.pct)	5	21	35	43
Cu-14Al-3Ni	82.85 69.38	14.15 27.90	3.00(wt.pct) 2.72(at.pct)	-82	-70	-60	-48

3.5 FACTORS AFFECTING THE TRANSFORMATION TEMPERATURES

a. M_s temperature is very sensitive to the alloy composition. A change in composition by as little as 1 wt.pct. would change the M_s temperature by as much as 100°C (Table VI).

TABLE VI - Transformation Temperatures of Some Cu-Al-Ni Alloys Changing with Composition.

No.	Composition(wt.pct)	M_s	M_f	A_s	A_f	Quenching Liquid	Ref.
		°C					
1	Cu-13.75Al-2.37Ni	21	5	35	43	10 pct caustic soda solution Q.	28
2	Cu-14.15Al-3.00Ni	-70	-82	-60	-48	"	28
3	Cu-14.09Al-2.97Ni	11	-10	30	45	"	28
4	Cu-14.00Al-4.20Ni	35	23	33	76	W.Q. at 0°C	7
5	Cu-14.10Al-4.20Ni	-20	-31	6	26	"	7
6	Cu-15.10Al-3.10Ni	-11	-	-	-	W.Q.	32
7	Cu-14.20Al-2.90Ni	146	-	-	-	W.Q.	32

b. M_s temperature is a function of quenching rate, M_s being lowered with increasing quenching rate. See Table VII.

TABLE VII - Transformation Temperatures of Some Cu-Al-Ni Alloys Changing with Quenching Rate.

No.	Composition(wt.pct)	M_s	M_f °C	A_s	A_f	Quenching Liquid	Ref.
1	Cu-14.20Al-4.30Ni	40-50	-	-	-	W.Q. at 100°C	31
2	Cu-14.20Al-4.30Ni	-10- -15	-	-	-	W.Q. at 20°C	31
3	Cu-14.10Al-4.20Ni	2.5	-11.5	20	38.5	W.Q. between 0°C to 50°C	16
4	Cu-14.10Al-4.20Ni	-18	-30	2	21		16
5	Cu-14.10Al-4.20Ni	-23	-42	2	14		16
6	Cu-14.10Al-4.20Ni	-28.5	-39	-4	10		16

IV. EXPERIMENTAL WORK AND RESULTS

The alloy Cu-Al-Ni was chosen for the present study because;

a. it is composed of a relatively inexpensive material than many of these exotic materials.

b. there is a major supportive literature on the transformation aspects of the alloy.

c. color changes are associated with the parent to martensite transformations (copper to bright yellow), which permit observer to detect its phase changes with the naked eye [9].

During production two main difficulties were encountered. Firstly, because the alloy is oxidized especially at high temperatures the specimens were heat-treated in evacuated steel tubes (Figure 29), and for other heat-treatments a horizontal tube furnace was prepared (Figure 30), through which a stream of argon gas was passed. The second difficulty encountered was the brittleness of the alloy. Therefore, the specimen for bending tests could not be prepared by referring to the common cutting techniques such as milling cutter, and the specimen was cut into suitable form by spark cutting (Figure 32).

Bending and hardness tests were carried out in parent and martensitic phases as well as hardness tests were performed after each stage of production.

A metallographic study was made of both etched surfaces and of unetched surfaces using incident light, polarized light, and interference phase contrast (IPC) system. All optical micrographs were taken at room temperature.

4.1 PRODUCTION OF A Cu-Al-Ni SYSTEM

4.1.1 Composition

The composition range over which the martensite transformation occurs with the M_s close to room temperature is 2 pct. to 3 pct. Ni by weight, 14 pct. aluminium and the remainder copper in nominal composition [28]. The strain memory effect was studied in Cu-14Al-3Ni (wt. pct.) alloy system having M_s close to room temperature. The reason for choosing this alloy which has M_s temperature around but a little below room temperature is to observe the structural changes without special equipments.

4.1.2 Melting and Casting

The alloy was prepared from 99.9 pct. Cu, 99.9 pct. Al, and 99.9 pct. Ni. Copper, aluminium, and nickel were supplied from Rabak, London and Scandinavian Metallurgical Co. Limited (England), and TUBITAK respectively. The required amounts of the metals were weighed to produce

the alloy with desired composition. Melting was done in a graphite crucible by the use of a medium frequency induction furnace under an argon atmosphere (Figure 28). The melt was cast into a Cu-mold(1.5x 9x11 cm^3) at 1200°C. The ingot was allowed to furnace-cool.

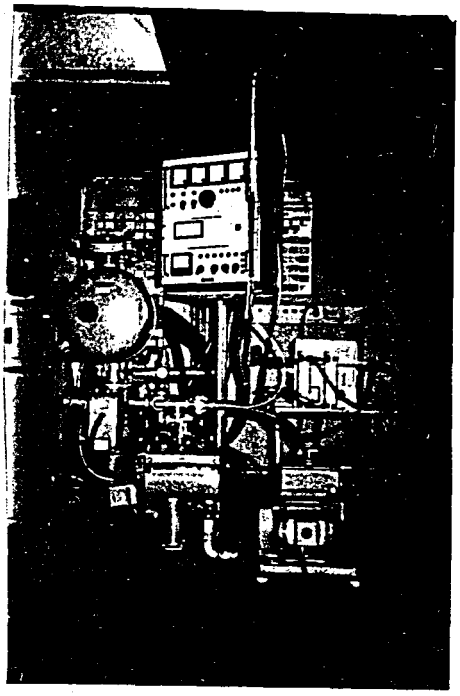

Figure 28 - Medium frequency induction furnace (Balzers).

4.1.3 Homogenization

The resulting ingot was heat-treated at 1000°C for 48 hours under vacuum to homogenize the structure, followed by furnace cooling. For this purpose a steel tube shown in Figure 29 was prepared and the ingot was placed in it. Then, to minimize high temperature oxidation it was evacuated to 10^{-2} torr vacuum by a vacuum pump. After that it was placed into an electric resistance heating furnace and kept for 48 hours. After homogenization treatment portions of the ingot were

chemically analyzed. Following the heat-treatment the ingot was machined to remove oxide surface layers.

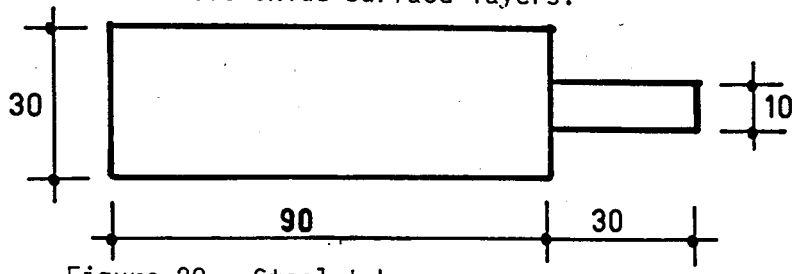

Figure 29 - Steel tube.
Dimensions are in mm.

4.1.4 Hot-rolling

After homogenization the ingot was hot-rolled at 950°C range from 15 mm to a thickness of 4 mm. The argon controlled furnace (Figure 30) was set close to the rolling mill (Figure 31) in order to be able to make the hot-rolling at appropriate temperature. The ingot was taken out of the furnace at 950°C and given to the rolling mill. This process was repeated three times.

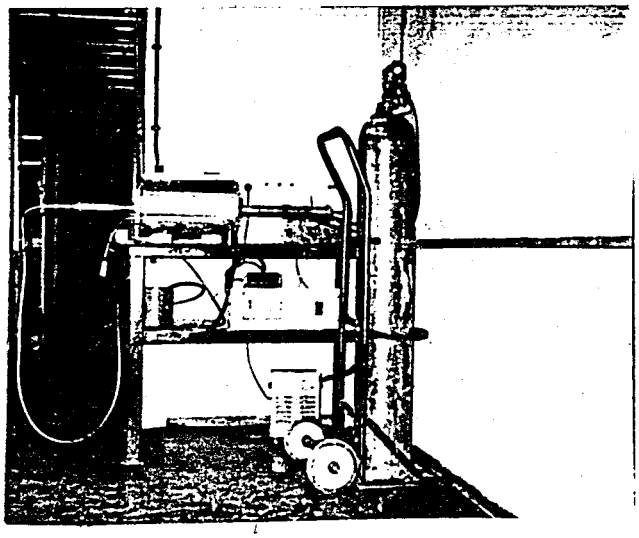

Figure 30 - Horizontal tube furnace.

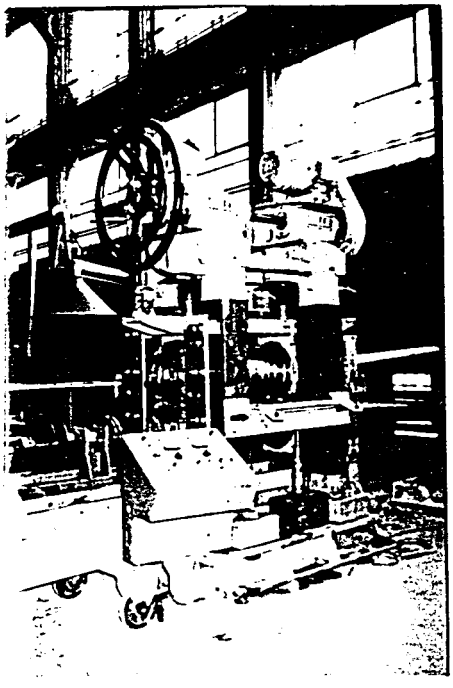

Figure 31 - Rolling mill.

4.1.5 Annealing and Quenching

The ingot was subsequently annealed at 900°C for four hours in the argon controlled furnace and then quenched into water at 17.5°C in order to retain β_1 matrix at room temperature.

4.2 DETERMINATION OF THE TRANSFORMATION TEMPERATURES

The martensitic transformation temperatures were measured by immersing the specimen in water and examining the microstructure whilst heating and cooling.

The alloy was put into a glass bowl containing water in which a thermometer was placed. Then ice parts were added one after another into the bowl to control the cooling rate. The appearance of the first martensite on the alloy was observed at about 10°C, which may be taken as M_s temperature. With decreasing temperature the already existing martensites grew larger in size and some other martensites nucleated in other parts of the alloy. When the surface of the alloy was covered with martensites completely the thermometer was checked and the temperature was 6°C, which may be taken as M_f temperature.

To obtain A_s and A_f temperatures, the same apparatus containing completely transformed alloy was heated with a hot plate. The temperature at which martensite started to disappear was 36°C, which is A_s. With continuous heating all the martensites on the alloy disappeared completely, at a temperature of 43°C, which is A_f.

Table VIII shows composition of polycrystalline material with the transformation temperatures.

TABLE VIII - Composition and Transformation Temperatures of Polycrystalline Material.

Nominal composition	Chemical analysis			°C			
	Cu	Al	Ni	M_s	M_f	A_s	A_f
Cu-14Al-3Ni(wt.pct.)	82±1	13.98	2.94	10	6	36	43

4.3 THREE-POINT BENDING TESTS

After quenching, bending test specimen was cut into suitable form by spark cutting (Figure 32). The dimensions of the specimen are given in Figure 33. Then, it was lightly mechanically polished without etching to observe the changes in the structure with naked eye during testing. It was again annealed at 900°C for a half an hour in the argon controlled furnace and quenched into water at 15°C to eliminate surface damages caused by mechanical polishing, followed by polishing with diamond paste. Bending tests were performed at room temperature.

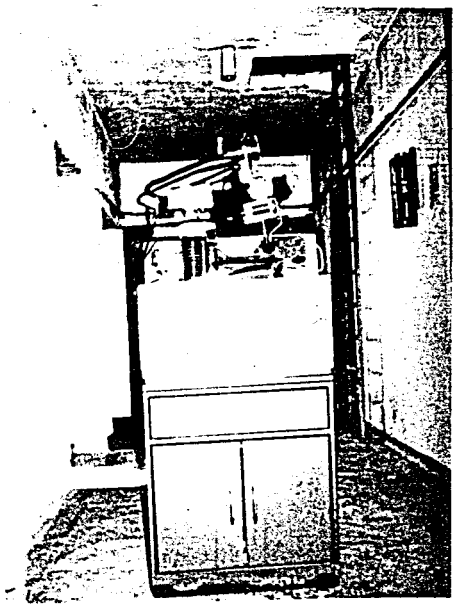

Figure 32 - Spark cutting machine (servomet).

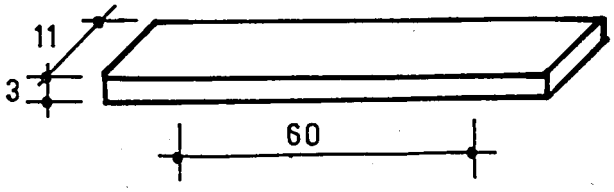

Figure 33 - Bending test specimen. Dimensions are in mm.

While preparing the specimen the standards were violated because of the difficulty of reducing the thickness during hot-rolling and the difficulty in machinability. Therefore, the following estimations were assumed:

$$\frac{\text{distance between supports}}{\text{thickness}} \simeq 20 \qquad \text{width} \simeq 4 \times \text{thickness}$$

An instron machine (TT-1115 type, Figure 34) was used during the tests at a cross-head speed of 0.5 mm per minute. Specimen was not normally taken to fracture but rather to fixed deflections of two and three mm in the parent and martensitic states. For each two states of the alloy four tests were performed by loading the specimen monotonically. During loading, the load vs deflection was recorded graphically (Figures 35-38). From the curves obtained, the maximum stress in the elastic region can be calculated from the following formula [33].

$$\text{Bending stress, } \sigma = 1.5 \frac{PL}{bh^2} \ (\text{kg/mm}^2)$$

where;

P = load,

L = length between supports,

b = specimen width,

h = specimen thickness.

Figure 34 - Instron machine, TT-1115 type.

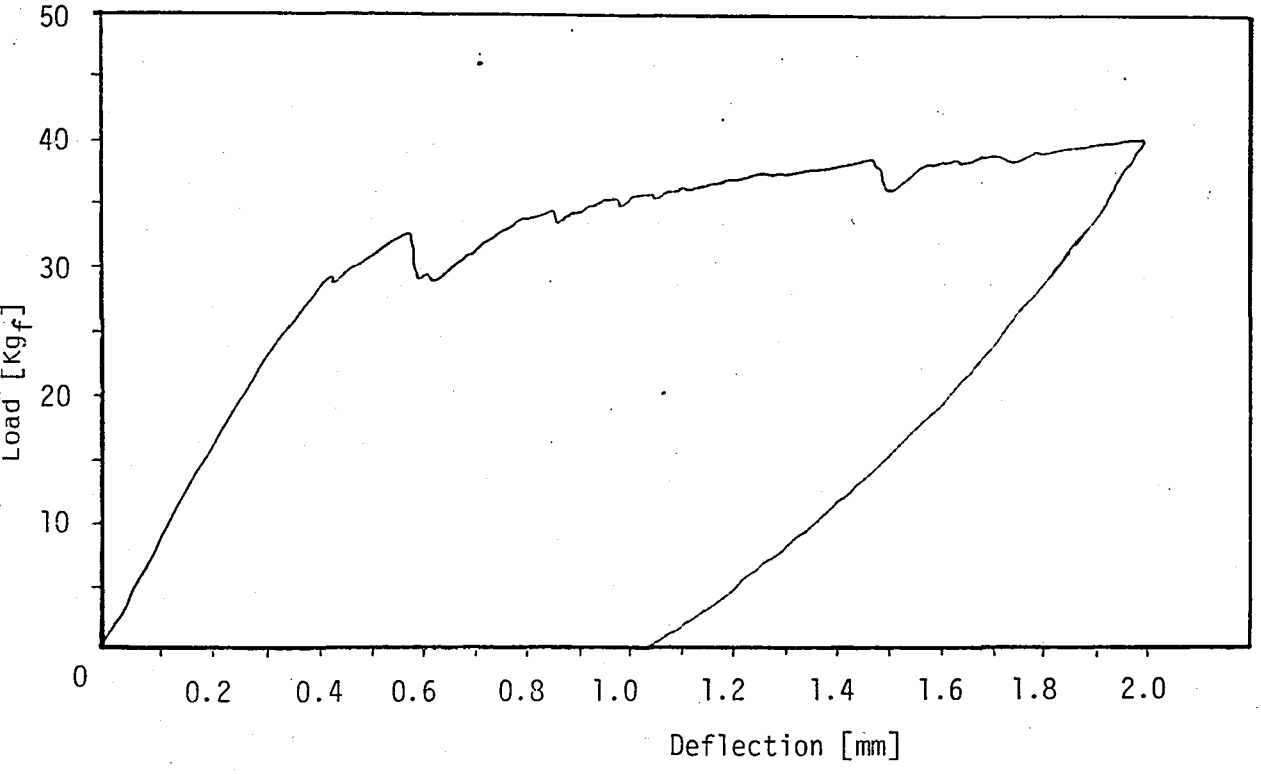

Figure 35 - Load-deflection curve by martensite formation obtained at room temperature. The residual deflection is completely recovered when the specimen is heated.

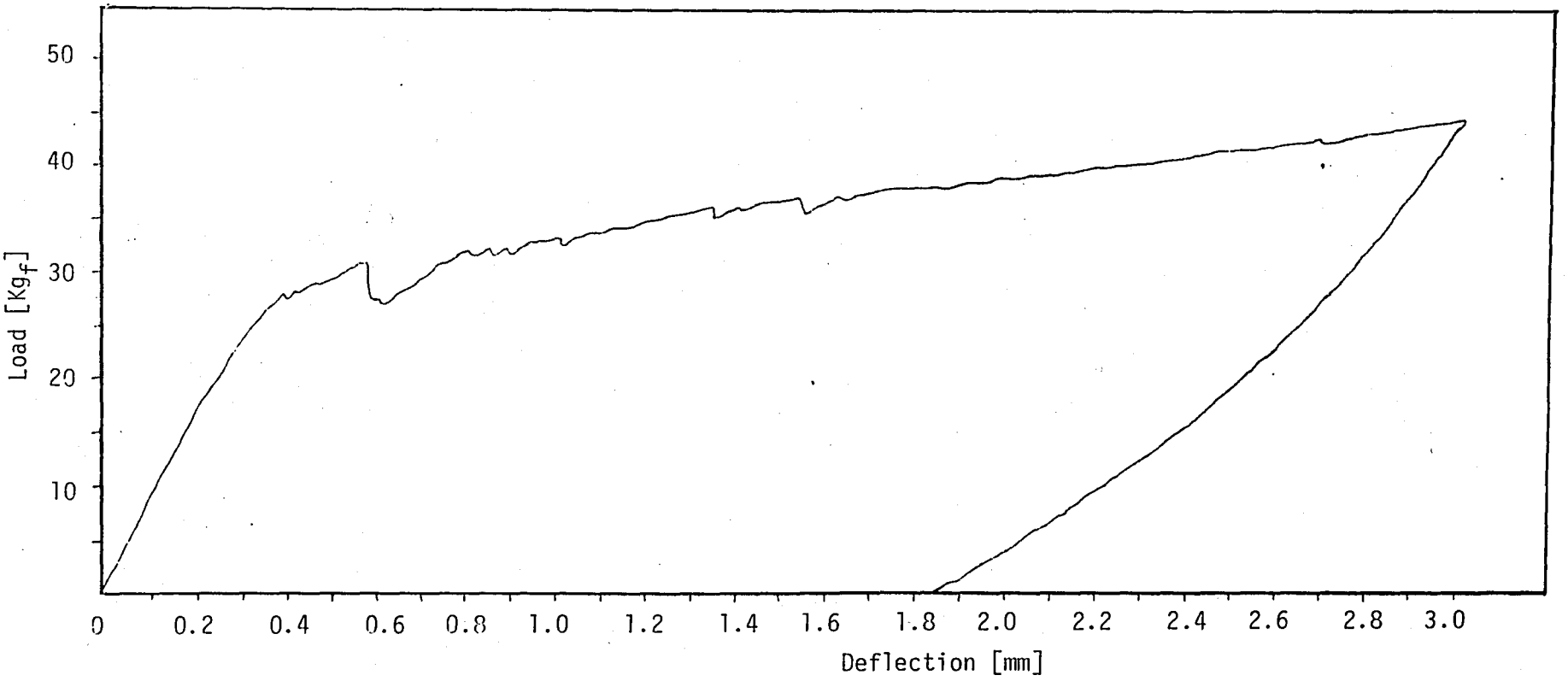

Figure 36 - Load-deflection curve by martensite formation obtained at room temperature. The residual deflection is completely recovered when the specimen is heated.

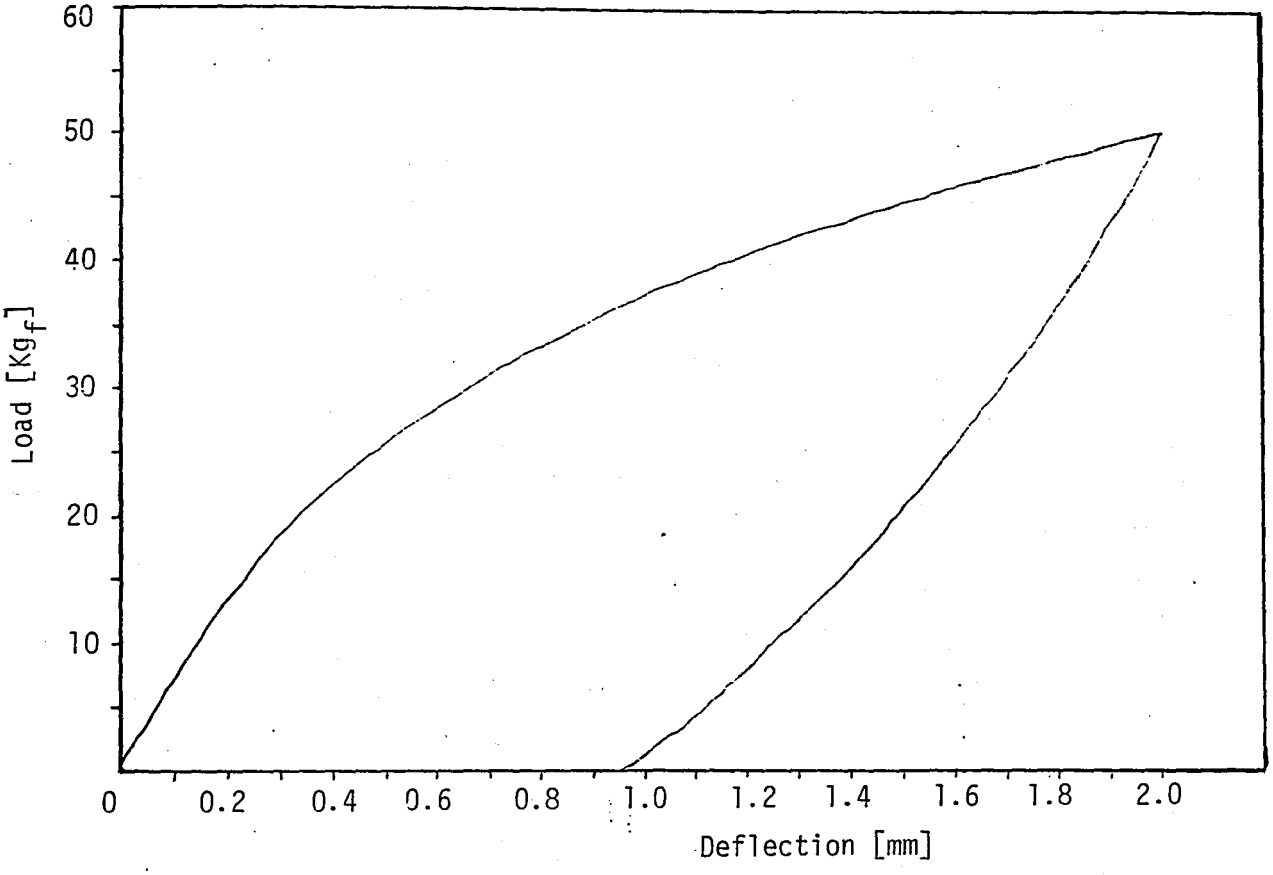

Figure 37 - Load-deflection curve by martensite reorientation obtained at room temperature. The residual deflection is completely recovered when the specimen is heated.

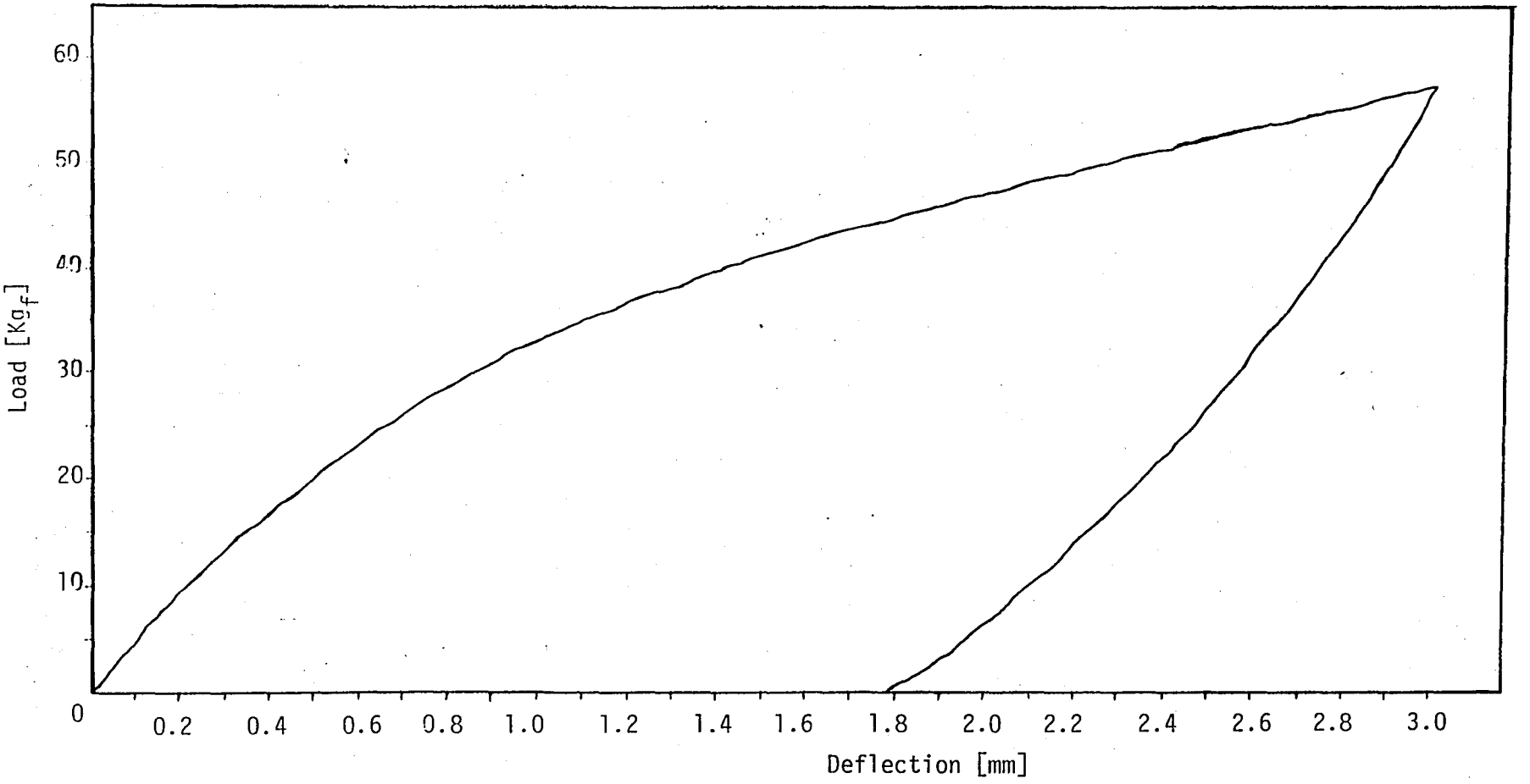

Figure 38 - Load-deflection curve by martensite reorientation obtained at room temperature. The residual deflection is completely recovered when the specimen is heated.

4.4 HARDNESS TESTS

Vickers-Brinell hardness tester (Figure 39) was used during tests. Specimens used for optical examinations were also used as hardness specimens.

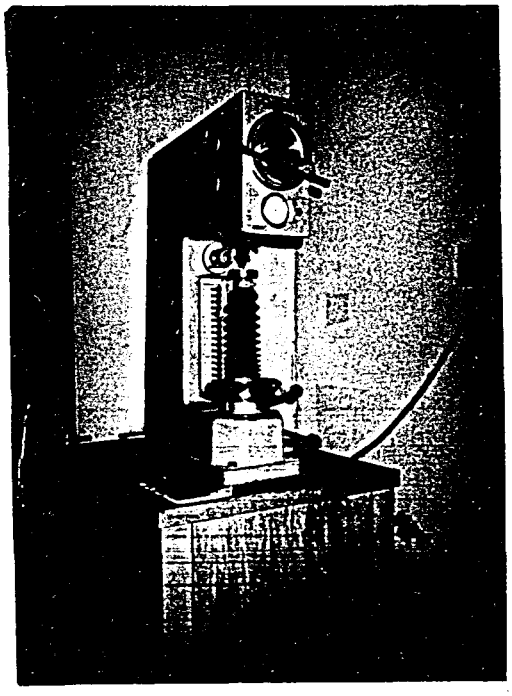

Figure 39 - Karl-Frank hardness test machine.

Vickers hardness tester uses a square base diamond pyramid as indenter and Vickers Hardness Number (VHN) is defined as the load divided by the surface area of the indentation which is calculated from microscopic measurements of the lengths of the diagonals of the impression.

$$VHN = 1.854P/L^2$$

where;

P = employed load,

$L = (d_1 + d_2)/2$,

d_1 = diagonal length,

d_2 = second diagonal length.

Five hardness tests were performed after casting, homogenization, hot-rolling, and quenching and in martensitic state at room temperature. 40 kgs load was employed for each testing to see the changes in hardness number at the same conditions. On one test specimen, three tests were made at different points, to obtain a correct mean hardness value. The hardness results are given in Table IX.

TABLE IX - Vickers Hardness Test Results at 40 kg Load.

State of the specimens	Readings of mark diameters			Average	Value of hardness (VHN/40 kg_f/30")
After casting	0.37	0.37	0.37	0.37	542
After homogenization following the casting	0.39	0.40	0.40	0.40	464
After hot-rolling following the homogenization	0.38	0.38	0.39	0.38	514
After quenching (Parent phase)	0.51	0.51	0.53	0.52	274
In the martensitic state	0.50	0.50	0.50	0.50	297

4.5 METALLOGRAPHIC EXAMINATION

4.5.1 Specimen Preparation

The microstructures of the alloy were investigated in detail under an optical microscope after careful polishing was performed. On mechanical polishing, emery papers of increasing fineness were used and this was followed by polishing with diamond paste, washing in water and then with alcohol, and finally drying in a stream of hot air. 2 g. $FeCl_3$, 10 cm^3 HCl, and 100 cm^3 H_2O solution was used as the etching reagent.

Reichert Metapan table microscope which is seen on the right side in Figure 40 was used for the microscopic examination of the specimens and microphotographs were taken by using Reichert MeF_2 Metallograph which is on the left in Figure 40.

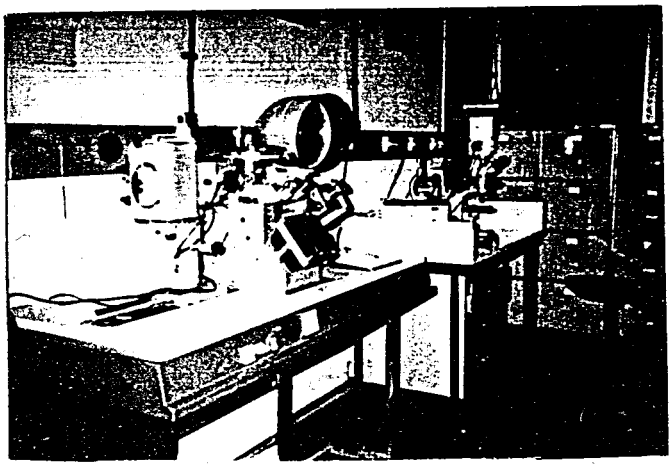

Figure 40 - Optical microscopes used in optical examinations (on the right) and taking micrographs.

4.5.2 Experimental Results

a. Microstructures of the Alloy During the Production Process

Figures 41, 42 and 43 show the microstructures of the alloy after casting, 48 hours homogenization at 1000°C, and hot-rolling at 950°C respectively. They were taken from different regions of the same specimen.

(a)

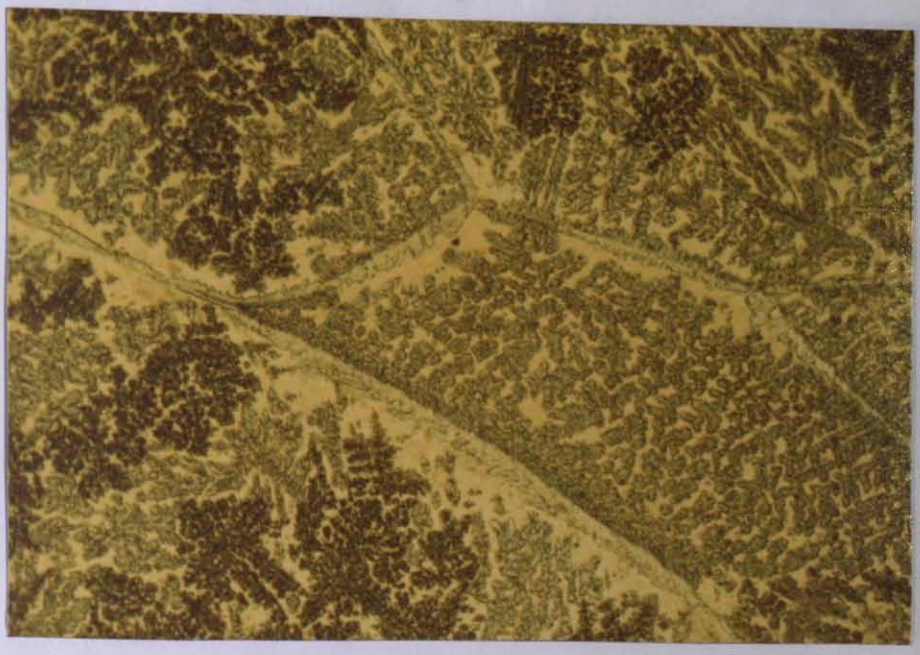

(b)

Figure 41 - The alloy after casting, etched, incident light. (a) Low magnification 62.5X. (b) High magnification 250X.

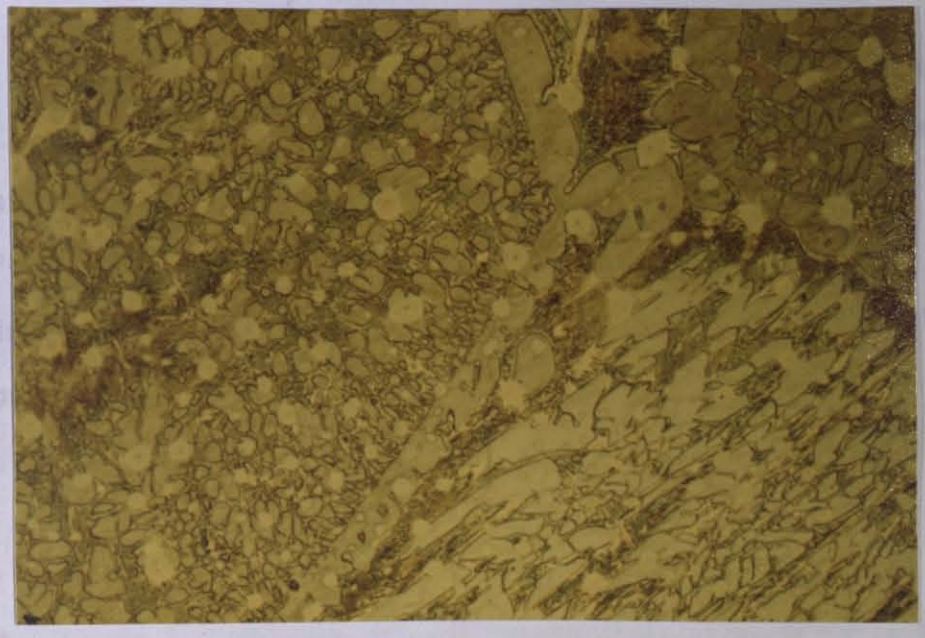

Figure 42 - After 48 hours homogenization at 1000°C, etched, incident light. High magnification 250X.

Figure 43 - After hot-rolling at 950°C, etched, incident light. High magnification 250X.

b. Microstructures of the Quenched Alloy

Figure 44 shows microstructures of the alloy quenched from 900°C into water. Figure 44(a) was taken from the specimen which was annealed at 900°C for four hours then quenched into water at 17.5°C. Figure 44(b) shows the parent phase structure of the specimen prepared for bending tests. It was heat-treated for half an hour followed by quenching into water at 15°C.

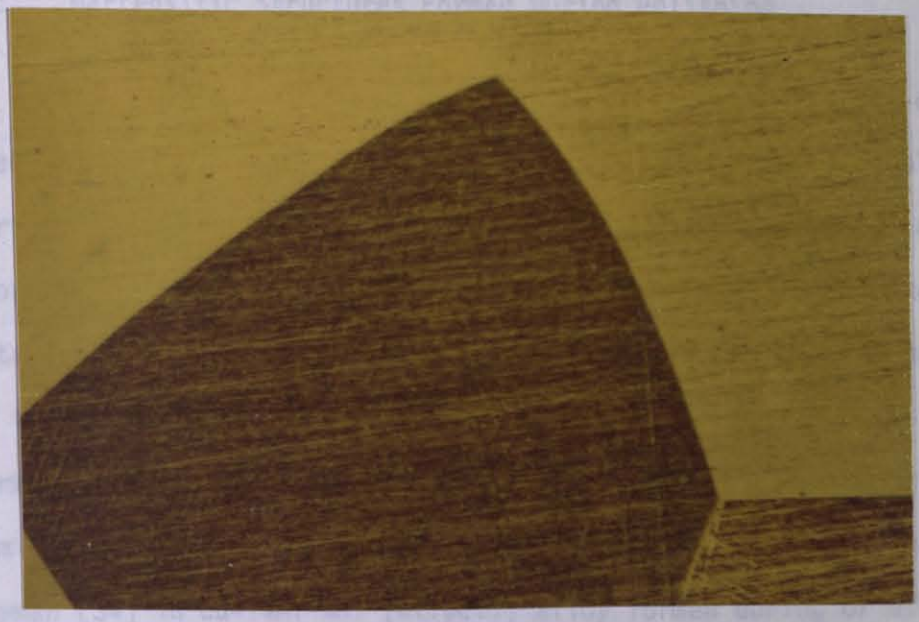

(a)

(b)

Figure 44 - Microstructures of the quenched alloy taken from different specimens. High magnification 250X. a) Etched, incident light (b) Unetched, interference phase contrast system.

c. Martensitic Structures Formed During Polishing

Figure 45 shows typical martensite structures of an as-quenched specimen into 17.5°C of the present alloy. Large spear-like plates of martensite are seen. Since the M_s temperature of the present alloy is about 10°C, which is below room temperature, and the spear-like martensite is observed only at the edges of the specimen with the sharp end of the spear running inward, it is possible that this martensite is formed by the assistance of stresses during mechanical polishing. The similar martensite structures have also been observed by Kuwano and Wayman [34] in Cu-14Al-4Ni (wt.pct.) alloy formed during or after electropolishing.

(a)

(b)

(c)

Figure 45 - Typical microstructures taken from the as-quenched specimen. Martensites formed during mechanical polishing. Unetched, low magnification 62.5X. (a) and (b) polarized light. (c) incident light.

d. Thermal Martensites

Figure 46 shows the γ_1' martensites in the present alloy system taken from bluk specimens by cooling them below their M_f temperature. The specimens were heat-treated at 900°C for half an hour and then quenched into water at 15°C before cooling them below M_f temperature. As seen in the figures, the size of the γ_1' martensites are quite large. They have a spear-like form and consist of two halves which are twin related to each other according to twinning plane. This property of them is more precisely shown in Figure 46(a). The spear-like form having twins inside itself is already a characteristic of Cu-Al-Ni alloys and have been investigated in detail [31].

(a)

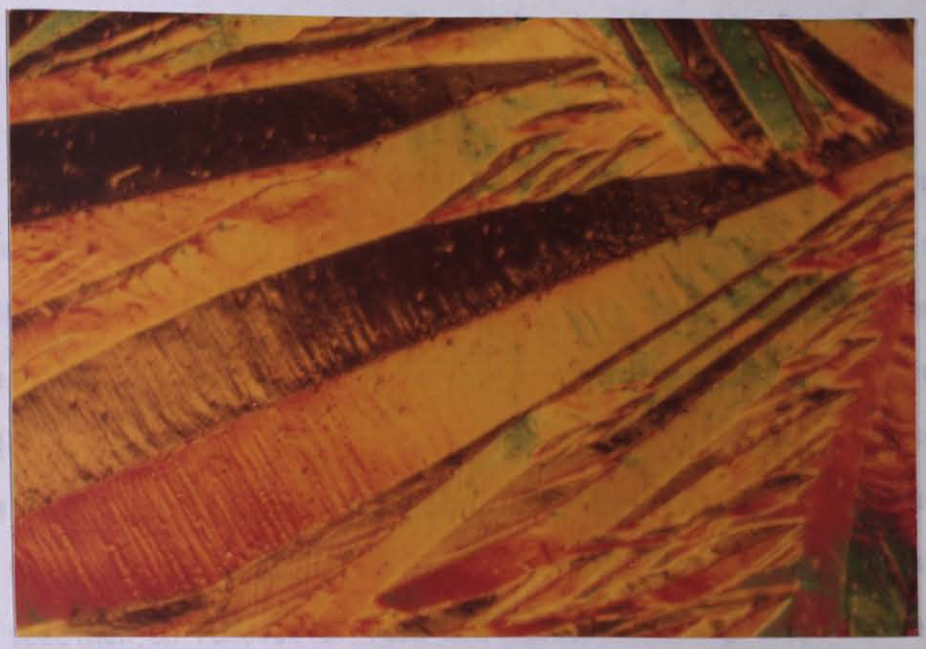

(b)

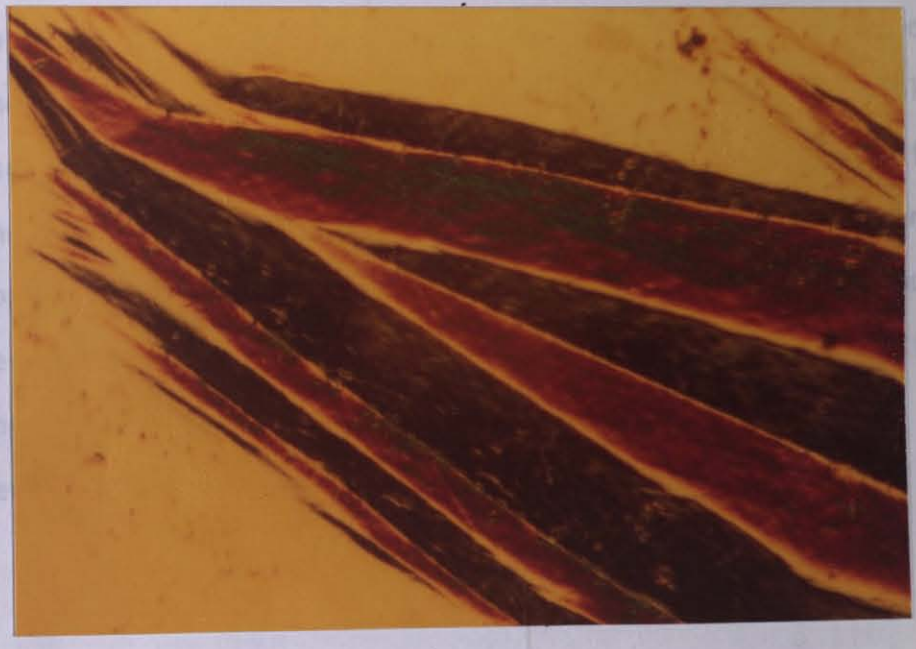

(c)

Figure 46 - Microstructures of thermally induced γ_1' martensite. Unetched, interference phase contrast system. a) Low magnification 62.5X. (b) Middle magnification 125X. (c) High magnification 250X.

e. Martensitic Structures Formed by Loading the Parent Phase

Typical morphological changes in the specimen with the load-deflection behaviour of Figures 35 and 36 at room temperature is shown in the series of micrographs of Figure 47. They were taken from the same area. Figure 47(a) represents initial stage before applying any load. Figure 47(b) shows the microstructure upon unloading after 2 mm deflection. As seen from the Figure 47(b) deformation caused the formation of martensite plates. Before Figure 47(c) was taken, the specimen on removal of load was heated above A_f temperature and thus reverted to the original β_1 phase (Figure 47(a)). Figure 47(c) corresponds to unloading after 3 mm deflection. It is seen that the amount of martensite increased - the more the specimen is deflected, the more the martensite plates nucleate and grow. Martensite plates are seen to exist even after unloading. However, when the specimen was heated above A_f temperature after two unloadings, the martensite disappeared and the specimen turned to its original position showing shape-memory effect (Figure 47(a)). From the comparison of optical micrographs, it is suggested that these martensites are the γ_1' martensites as has been determined by Otsuka et al. [16,25].

(a)

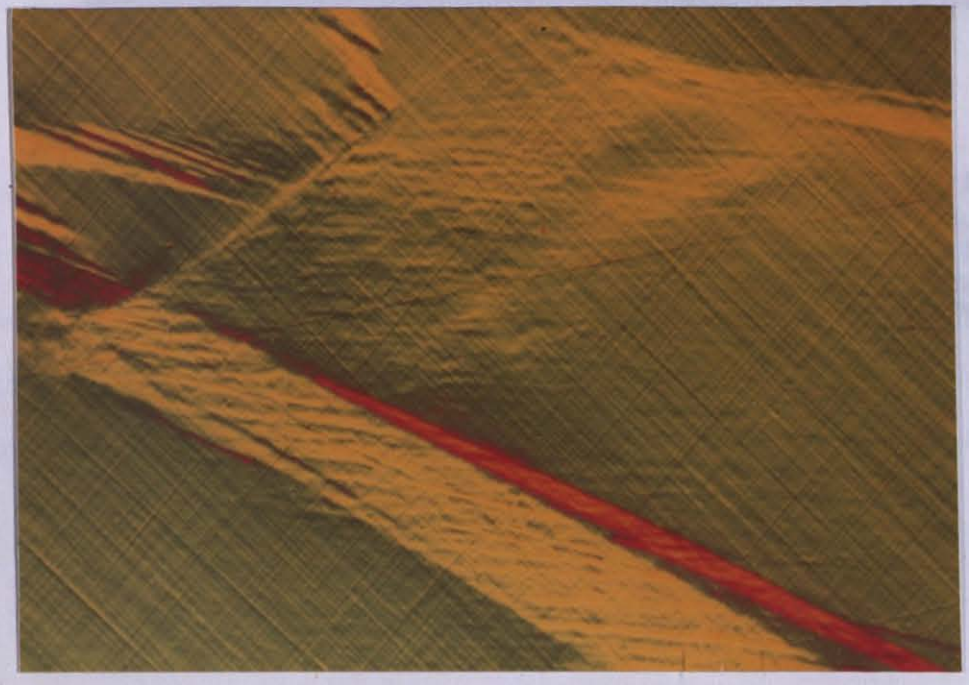

(b)

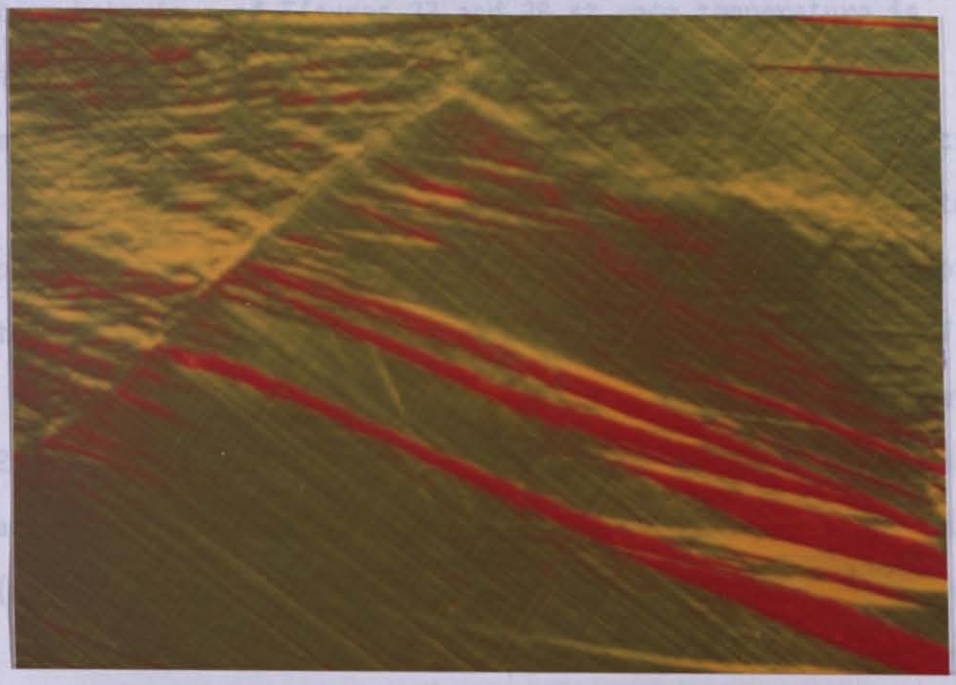

(c)

Figure 47 - The microstructures associated with Figures 35 and 36. Unetched, interference phase contrast system, high magnification 250X. (a) The microstructure of the specimen in the undeformed state (parent phase). (b) After 2 mm deflection.(c) After 3 mm deflection.

f. Reorientation of the Thermally Induced Martensite

Typical morphological change in the specimen with the load-deflection behaviour of Figures 37 and 38 at room temperature is shown in the series of micrographs of Figure 48. The specimens had a martensitic structure before commencing the tests. The micrographs were taken from the same area. Figure 48(a) shows the martensitic phase (thermal martensites) before loading. Figure 48(b) corresponds to microstructure taken after unloading preceded by 2 mm deflection. Before applying the second deflection, the deformed specimen after 2 mm deflection was straightened out by heating it between the temperatures ranging from A_s to A_f, reproducing the straight parent phase (β_1). Then, it was again cooled below its M_s temperature producing the thermal martensite state (γ_1') which is the original martensitic phase structure. After it was turned to its original position it was given a deflection of 3 mm. The micrograph was taken after unloading (Figure 48(c)). The deformed specimens in both kinds of deflection returned to its original β_1 state, Figure 48(d), on heating above A_f showing usual kind of shape-memory effect. As reported by Otsuka [10] and according to the optical examinations, the structures formed after different deflections are also the γ_1' martensite plates.

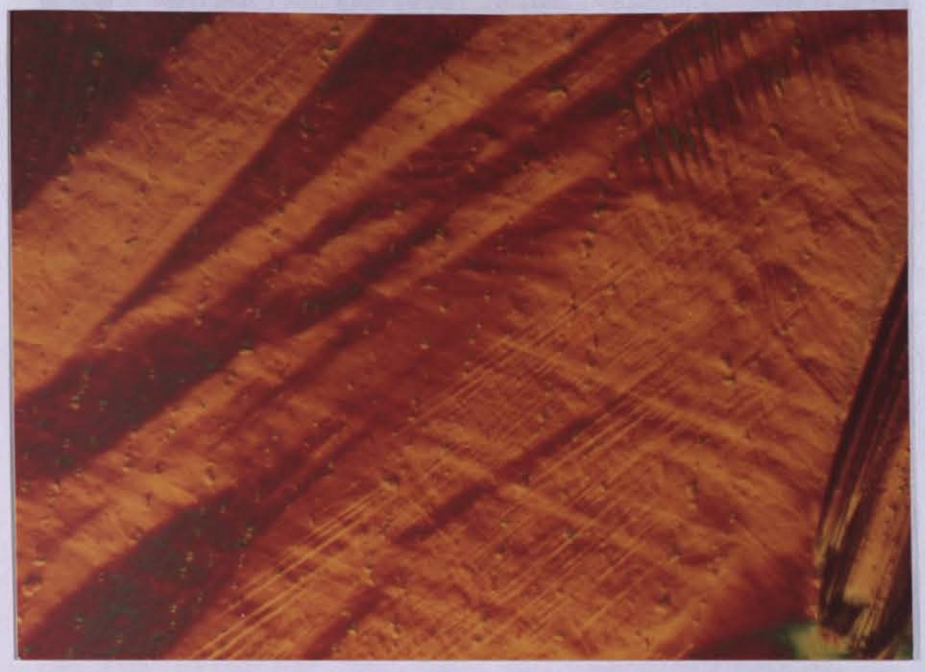

(a)

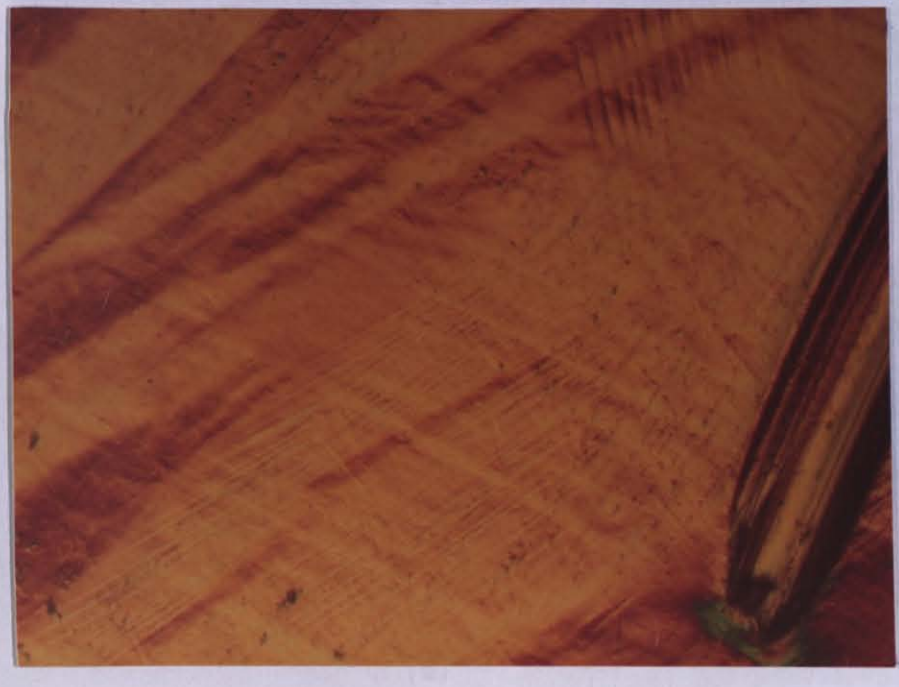

(b)

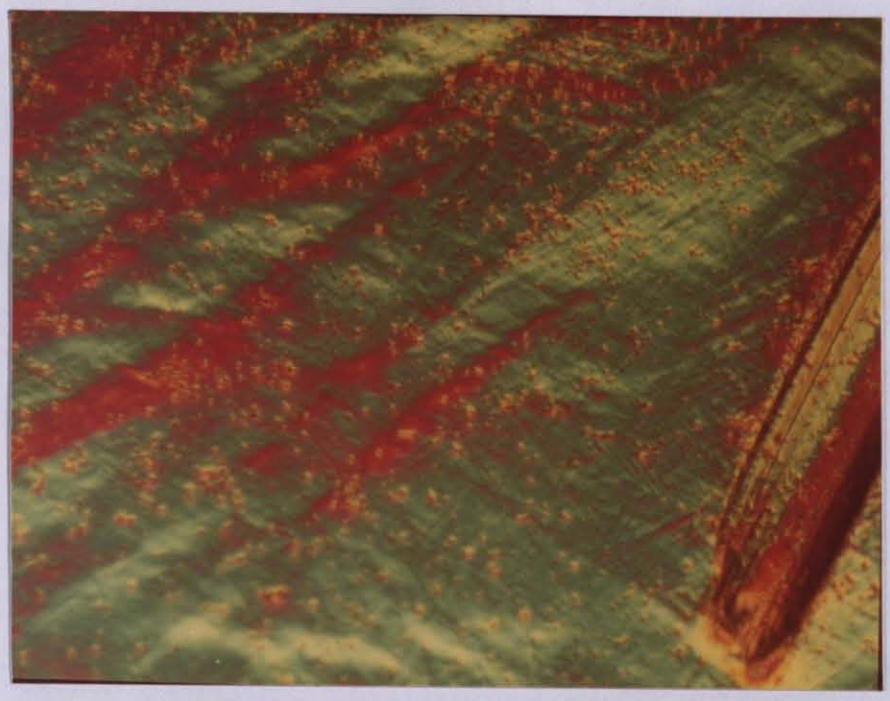

(c)

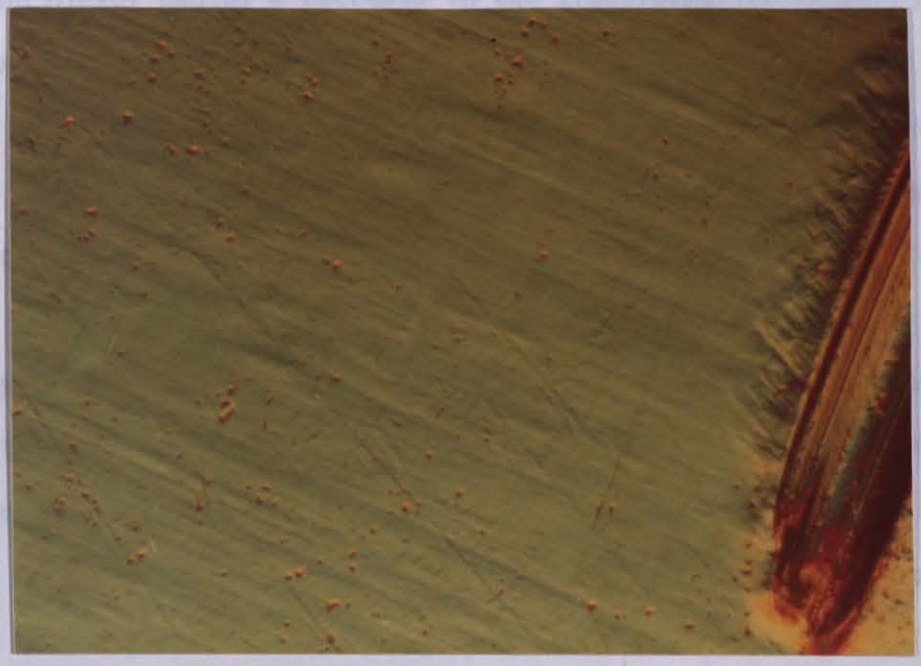

(d)

Figure 48 - The microstructures associated with Figures 37 and 38. Unetched, interferene phase contrast system, high magnification 250X. (a) The microstructure of the specimen in the undeformend state (Martensitic phase). (b) After 2 mm deflection.(c) After 3 mm deflection. (d) Original parent phase.

V. DISCUSSION

5.1 ON THE TRANSFORMATION TEMPERATURES

A close inquisition of the Table VI to understand the nature of transformation temperatures of some alloys changing according to compositions shows that the increase in the amount of aluminium (Figure 18) and nickel causes a decrease in the transformation temperature. For example, a comparison of compositions,number four and five in Table VI exhibits that the 0.1 pct. increase in the amount of aluminium gives rise to a decrease of 55°C in M_s temperature. To see the result of increase in the amount of nickel, one can make a comparison between alloy seven in Table VI and alloy two in Table VII. They both have nearly the same quenching conditions. The 1.4 pct. increase in the amount of nickel causes approximately a decrease of 156-161°C in M_s temperature.

A comparison of the transformation temperatures of the present alloy to alloy three in Table VI and the alloy (Cu-14Al-3.4Ni (wt.pct.)) given in reference 35 shows that they have similar transformation temperatures, although there are some changes in compositions. Perhaps the reason for this similarity is that they have some differences in

their quenching rates. Transformation temperatures change with quenching rate as shown in Table VII. Since a dilatometer has not been used in obtaining the transformation temperatures of the alloy studied in this work, there might also be some errors in these values obtained only by the naked eye.

5.2 ON THE HARDNESS TESTS

An observation of the values of hardness obtained in Table IX shows that the value of hardness is 542 VHN after casting process. The homogenization of the alloy after casting causes a decrease in the hardness value (464 VHN) but after it is hot-rolled, an increase in the hardness is again observed (514 VHN). When the alloy is quenched, a considerable decrease dropping to 274 VHN is seen. After all these processes, cooling the specimen below its M_f temperature gives rise to a small increase in the hardness reaching to 297 VHN.

The deformation characteristics of shape-memory alloys are such that even intrinsically brittle austenitic materials may be rendered ductile by transformation to martensite [11]. For example, martensitic CuZn is extremely ductile, whereas the parent β-brass is comparatively brittle. The same holds for Ni-Ti alloys. Although CuZn and Ni-Ti alloys exhibit ductility in the martensitic phase the present alloy still remains in its brittle nature.

5.3 ON THE LOAD-DEFLECTION CURVES AND METALLOGRAPHY

It is well established that alloys near Cu_3Al transform from the β_1 matrix phase (DO_3 type ordered structure) to the γ_1' martensite phase (2H structure in Ramsdell notation) when they are cooled below the M_s temperature [16,30,31]. For the present alloy, the room temperature is between the M_s and A_s. So quenching from 900°C into water retained the β_1 phase (Figure 44), which on subsequent cooling below M_s transformed to γ_1' martensite as shown in Figure 46. Deformation of the β_1 and γ_1' phases at ambient temperature resulted in formation and reorientation of the martensite. The structure formed after deformation of the β_1 and γ_1' phases was also the γ_1' martensite which was stable on removal of the load [10,16,25]. The martensite structure formed in both states converted to the parent phase structure after heating to A_f (Figures 47 and 48). The product γ_1' phase formed in all cases consists of parallel spear-like bands. However, only main bands resulting from the first shear have been observed and the sub-bands indicating the second shear of transformation (internal twins) have not been observed except Figure 46(a). As seen from the figure, two martensite plates on the right contain internal twins inside them. To be able to get better results from the micrographs interference phase contrast (IPC) system was used in conjunction with Reichert MeF2 Metallograph.

To reveal microstructural changes upon deformation, specimens were observed in sequence after each deformation process under an optical microscope. Since deformation modes depend upon the state of specimen, i.e. whether the specimen was transformed or not, it was examined in two different states; (I) in an untransformed state, and (II) in a transformed state.

Due to the lack of equipment it could not be possible to observe the microstructures while deforming the specimen. Therefore, the load-deflection curves obtained will be discussed by referring to some specific references [16,25,28].

5.3.1 Memory Effect - Case I

Typical load-deflection curves as a function of deflection are shown in Figures 35 and 36. With increasing load from an initial zero no morphological change occurs up to the point (~27 kg_f or~25 kg/mm^2) where further loading causes martensite plates to form. This linear portion represents elastic deformation of the matrix β_1. Stress induced martensite is formed above the stated critical stress and serrations suddenly appear in the curve above this value of the stress. The rapid movement of the interfaces is associated with the drop in the load as shown in the load-deflection curves. With increasing deflection the load level does not change much and the specimen appears to elongate plastically, as if it were being permanently deformed. Once the martensite has formed it is thermodynamically stable even on removal of load and it is necessary to heat the specimen to A_s in order for the martensite to start to revert to the β_1 phase. Figure 47 shows the microstructures after 2 mm and 3 mm deflections. With increasing load, the region of martensite in the grain expands and other martensites nucleate. This observation is consistent with the results of Oishi and Brown [28] (Figure 27).

5.3.2 Memory Effect - Case II

The load-deflection curves are shown in Figures 37 and 38. In this state martensite are present from the start. Thus mobile lattice defects such as boundaries between martensite and the matrix or internal twins are present which cause plastic deformation even at very low load levels (~14 kg_f or ~13 kg/mm^2) and decreases the elastic deformation region compared to case (I). Deflection causes reorientation of already existing martensite plates such that favorably oriented martensite plates grow at the expense of unfavorably oriented ones (Figure 48). There is a permanent set on removal of the load. The specimen deformed in the martensitic state still showed essentially complete recovery. Thus, when the deformed martensite is heated into β_1 phase region the specimen reverts to the length it originally had in the martensitic state before loading.

Depending on the optical microscope examinations and microphotographs the following characteristics in morphology, and the test temperature indicate that γ_1' martensite is formed by cooling below M_f or under load (in both cases, (I) and (II)).

a. Spear-like form;
b. Presence of internal twins which is characteristic of the γ_1' martensite;
c. Occurrence of bending process in the range of $A_s > T > M_s$.

VI. CONCLUSION

i. For the present alloy, room temperature is between M_s and A_s. Therefore, specimens can be deformed either in the martensitic state or in the β_1 state at room temperature where the martensite once formed is stable. In the latter case, deflection causes the formation of martensite plates with preferred orientation, whilst loading in the martensitic state causes reorientation of already existing martensite plates. Specimens originally in the β_1 state return to their original length on heating above A_f.

ii. In the curves obtained, the yield stress of the martensite (~13 kg/mm^2) is lower than those deformed in the parent phase condition (~25 kg/mm^2).

iii. The curves obtained in the β_1 case show a load plateau after yielding.

iv. In spite of the fact that even intrinsically brittle austenitic materials may be rendered ductile by transformation to martensite the present alloy keeps its brittle nature.

BIBLIOGRAPHY

1. Perkins, J., "Shape-Memory Behaviour and Thermoelastic Martensitic Transformations", Materials Science and Engineering,Vol. 51, pp. 181-192, 1981.

2. Schetky, L. McDonald, "Shape-Memory Alloys", Scientific American, Vol. 241, pp. 74-82, 1979.

3. Delaey, L., Krishnan, R.V., Tas, H., and Warlimont, H., "Thermoelasticity, Pseudoelasticity and the Memory Effects Associated with Martensitic Transformations", Journal of Materials Science, Vol. 9, pp.1521-1555, 1974.

4. Duerig, T.W., Albrecht, J., and Gessinger, G.H., "A Shape-Memory Alloy for High-Temperature Applications", Journal of Metals, pp. 14-20, December 1982.

5. Perkins, J., and Sponholz, R.O., "Stress-Induced Martensitic Transformation Cycling and Two-Way Shape-Memory Training in Cu-Zn-Al Alloys", Metallurgical Transactions A, Vol. 15A, pp. 313-321, February 1984.

6. Schroeder, T.A., and Wayman, C.M., "Pseudoelastic Effects in Cu-Zn Single Crystals", Acta Metallurgica, Vol. 27, pp. 405-417, 1979.

7. Otsuka, K., Sakamoto, H., and Shimizu, K., "Successive Stress-Induced Martensitic Transformations and Associated Transformation Pseudoelasticity in Cu-Al-Ni Alloys", Acta Metallurgica, Vol. 27, pp. 585-601, 1979.

8. Wayman, C.M., "Some Applications of Shape-Memory Alloys", Journal of Metals, Vol. 32, No. 6, pp. 129-137, January 1980.

9. Otsuka, K., and Shimizu, K., "Memory Effect and Thermoelastic Martensite Transformation in Cu-Al-Ni Alloy", Scripta Metallurgica, Vol. 4, pp. 469-472, 1979.

10. Otsuka, K., "Origin of Memory Effect in Cu-Al-Ni Alloy", Japanese Journal of Applied Physics, Vol. 10, No. 5, pp. 571-579, May 1971.

11. Wayman, C.M., and Shimizu, K., "The Shape Memory ('Marmem') Effect in Alloys", Metal Science Journal, Vol. 6, pp. 175-183, 1972.

12. Perkins, J., "Martensitic Substructural Prerequisites for Shape-Memory Effect (SME) Behaviour", Scripta Metallurgica, Vol. 9, pp. 121-128, 1975.

13. Chakravorty, S., and Wayman, C.M., "The Thermoelastic Martensitic Transformation in β' Ni-Al Alloys: 1. Crystallography and Morphology", Metallurgical Transactions A, Vol. 7A, pp. 555-568, April 1976.

14. Nagasawa, A., Enami, K., Ishino, Y., Abe, Y., and Nenno, S., "Reversible Shape-Memory Effect", Scripta Metallurgica, Vol. 8, pp. 1055-1060, 1974.

15. Otsuka, K., Shimizu, K., "Stress and Strain Induced Martensitic Transformations", Proceedings of the International Conference on Martensitic Transformations, M.I.T., Cambridge, MA, pp. 607-618, June 1979.

16. Otsuka, K., Wayman, C.M., Nakai, K., Sakamoto, H., and Shimizu, K., "Superelasticity Effects and Stress-Induced Martensitic Transformations in Cu-Al-Ni Alloys", Acta Metallurgica, Vol. 24, pp. 207-226, 1976.

17. Wayman, C.M., "Thermoelastic Martensitic Transformations and the Shape-Memory Effect", Invited Paper Presented at AIME Annual Meeting, New York City, February 1985.

18. Schroeder, T.A., and Wayman, C.M., "The Two-Way Shape-Memory Effect and Other Training Phenomena in Cu-Zn Single Crystals", Scripta Metallurgica, Vol. 11, pp. 225-230, 1977.

19. Saburi, T., Nenno, S., and Wayman, C.M., "Shape-Memory Mechanism in Alloys", Proceedings of the International Conference on Martensitic Transformations, M.I.T., Cambridge, MA, pp. 619,632, June 1979.

20. Foxboro Corporation, Foxboro, Massachusetts, 02035, Technical Information Sheets on Nitinol Pen Drive Unit.

21. Ginell, W.S., McNichols, J.L., Jr., and Cory, J.S., "Nitinol Heat Engines", Mechanical Engineering, pp. 28-33, May 1979.

22. Andreasen, G.F., and Morrow, R.E., "Laboratory and Clinical Analysis of Nitinol Wire", American Journal of Orthodontics, Vol. 73, No. 2, pp. 142-151, 1978.

23. Netsu, N., Iwabuchi, T., and Honma, T., "A Study of the TiNi Intracranial Aneurysm Clip Having the Shape-Memory Effect", Bulletin of the Research Institute of Mineral Dressing and Metallurgy, Thoku University, Sendai, Japan, Vol. 34, pp. 67-73, 1978.

24. Sawyer, P.N., et al., "Further Study of Nitinol Wire as Contractile Artificial Muscle for an Artificial Heart", Bulletin of the Texas Heart Institute, Vol. 3, No. 1, pp. 65-68, 1976.

25. Otsuka, K., Nakai, K., and Shimizu, K., "Structure Dependence of Superelasticity in Cu-Al-Ni Alloy", Scripta Metallurgica, Vol. 8, pp. 913-918, 1974.

26. Otsuka, K., Nakai, K., and Shimizu, K., "Two Stage Superelasticity Associated with Successive Martensite-to-Martensite Transformations", Scripta Metallurgica, Vol. 10, pp. 983-988, 1976.

27. Otsuka, K., Sakamoto, H., and Shimizu, K., "Martensitic Transformations Between Martensites in a Cu-Al-Ni Alloy", Scripta Metallurgica, Vol. 9, pp. 491-498, 1975.

28. Oishi, K., and Brown, L.C., "Stress Induced Martensite Formation in Cu-Al-Ni Alloys", Metallurgical Transactions, Vol. 2, pp. 1971-1977, 1971.

29. Otsuka, K., Shimizu, K., Corneils, I., and Wayman, C.M., "Shape Recovery Temperature Range in Cu-Al-Ni and Cu-Zn Marmem Alloys", Scripta Metallurgica, Vol. 6, pp. 377-382, 1972.

30. Dvorack, M.A. et al., "Decomposition of a β_1-Phase Cu-Al-Ni Alloy at Elevated Temperature", Scripta Metallurgica, Vol. 17, pp. 1333-1336, 1983.

31. Otsuka, K., and Shimizu, K., "Morphology and Crystallography of Thermoelastic γ_1' Cu-Al-Ni Martensite", Japanese Journal of Applied Physics, Vol. 8, No. 10, pp. 1196-1204, October 1969.

32. Kennon, N.F., Dunne, D.P., and Middleton, L., "Aging Effects in Cu-Based Shape-Memory Alloys", Metallurgical Transactions A, Vol. 13A, pp. 551-555, April 1982.

33. Shigley, J.E., Mitchell, L.D., Mechanical Engineering Design, 4th Ed., Tokyo: Kosaido Printing Co., 1983.

34. Kuwano, N., and Wayman, C.M., "Some Effects of Parent Phase Aging on the Martensitic Transformation in a Cu-Al-Ni Shape-Memory Alloy", Metallurgical Transactions A, Vol. 15A. pp. 621-626, April 1984.

35. Kennon, N.F., and Dunne, D.P., "Shape Strains Associated with Thermally Induced and Stress Induced Martensite in a Cu-Al-Ni Shape-Memory Alloy", Acta Metallurgica, Vol. 30, pp. 429-435, 1982.